

**DEVELOPMENT AND PERFORMANCE EVALUATION OF CAU-1
METAL-ORGANIC FRAMEWORK /POLYETHER IMIDE MIXED
MATRIX MEMBRANE FOR GAS SEPARATION**

BY

Omar Waqas Saadi

A Thesis Presented to the
DEANSHIP OF GRADUATE STUDIES

KING FAHD UNIVERSITY OF PETROLEUM & MINERALS

DHAHRAN, SAUDI ARABIA

In Partial Fulfillment of the
Requirements for the Degree of

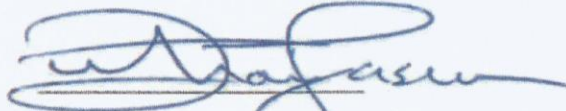
MASTER OF SCIENCE

In
MATERIALS SCIENCE AND ENGINEERING

December, 2017

KING FAHD UNIVERSITY OF PETROLEUM & MINERALS
DHAHRAN- 31261, SAUDI ARABIA
DEANSHIP OF GRADUATE STUDIES

This thesis, written by **Omar Waqas Saadi** under the direction his thesis advisor and approved by his thesis committee, has been presented and accepted by the Dean of Graduate Studies, in partial fulfillment of the requirements for the degree of **MASTER OF SCIENCE IN MATERIALS SCIENCE & ENGINEERING**.



Dr. Zuhair M. A. Gasem
Department Chairman



Dr. Salam A. Zummo
Dean of Graduate Studies



16/5/13
Date



Dr. Tahar Laoui
(Advisor)



Dr. Zafarullah Khan
(Member)



Dr. Bassem Maythalony
(Member)

© Omar Waqas Saadi

2017

Dedicated to my parents.

Saad ul Hassan and Shahnaz Saadi

ACKNOWLEDGMENTS

Foremost, I would like to express my sincere gratitude to my advisor Prof. Tahar Laoui for the continuous support of my MS study and research, for his patience, motivation, enthusiasm, and immense knowledge. His guidance helped me in all the time of research and writing of this thesis. I could not have imagined having a better advisor and mentor for my MS study.

Besides my advisor, I would like to thank the rest of my thesis committee: Dr. Bassem Almaythalony, and Dr. Zafarullah Khan for their encouragement, insightful comments, and hard questions.

My sincere thanks also go to Dr. Abbas Hakeem for offering me work opportunities in his group and leading me working on diverse exciting projects.

I thank my fellow lab mates in Carbon Capture Center: Dr. Usman, Muhammad Faizan, Mr. Mahmoud, and Ahmed Alloush for the stimulating discussions, for the sleepless nights we were working together before deadlines, and for all the fun we have had in the last three years.

Last but not the least, I would like to thank my family: my parents for giving birth to me at the first place and supporting me spiritually throughout my life.

TABLE OF CONTENTS

ACKNOWLEDGMENTS	V
TABLE OF CONTENTS	VI
LIST OF TABLES.....	IX
LIST OF FIGURES.....	X
LIST OF ABBREVIATIONS.....	XIII
ABSTRACT.....	XIV
ملخص الرسالة	XVI
1 INTRODUCTION.....	1
1.1 Flue gas	2
1.2 Natural gas.....	2
1.3 Responses to global warming.....	3
1.3.1 Mitigation.....	3
1.3.2 Adaptation	3
1.3.3 Climate Engineering.....	3
2 LITERATURE REVIEW	4
2.1 Swing adsorption techniques	4
2.1.1 Pressure swing adsorption	4
2.1.2 Vacuum swing adsorption	4
2.1.3 Temperature swing adsorption	4
2.2 Cryogenic distillation	5
2.3 Membrane gas separation	5

2.3.1	Non-Porous membranes.....	5
2.3.2	Porous membranes	5
2.4	Membrane separation properties	6
2.4.1	Permeability	6
2.4.2	Permeation flux.....	7
2.4.3	Selectivity (Separation factor)	7
2.5	Metal-Organic Framework membranes	7
2.6	Mixed-matrix membranes.....	10
2.7	Thesis Aim/Objectives	19
3	EXPERIMENTAL WORK.....	20
3.1	Synthesis of CAU-1	20
3.2	Preparation of CAU-1/PEI membrane	22
3.3	Characterization.....	24
3.4	Gas separation analysis.....	26
4	RESULTS AND DISCUSSION.....	28
4.1	CAU-1 Characterization	28
4.1.1	Powder X-ray Diffraction (XRD)	28
4.1.2	BET analysis	30
4.1.3	Sorption analysis	30
4.1.4	Scanning electron microscopy (SEM)	32
4.1.5	Thermogravimetric analysis (TGA).....	34
4.2	Mixed matrix membrane characterization	35
4.2.1	Microstructure	35
4.2.2	X-ray diffraction analysis	40

4.2.3	Gas Separation	41
4.2.4	Comparative analysis	47
5	CONCLUSIONS AND RECOMMENDATIONS.....	51
	REFERENCES.....	53
	VITAE.....	61

LIST OF TABLES

Table 1. Mechanical properties of AC/PEI MMMs [52]	14
Table 2. Gas permeability, ideal selectivity of MIL53 and NH2-MIL53 with Matrimid and Ultem mixed matrix membranes [52]	16
Table 3. Permeability P (Barrer) and selectivity α of different mixed matrix membranes from the literature	18
Table 4. Concentration of CAU-1 particles and PEI used to synthesise different membranes	22
Table 5. Permeabilities (Barrer) of mixed matrix membranes with different CAU-1 concentration for different gases at 35 C and 2.05 bar	43
Table 6. Ideal selectivity for different gas pairs for hydrogen separation	44
Table 7. Ideal selectivity for CO ₂ separation from N ₂ and CH ₄	44
Table 8. Diffusivity of different gases as a function of CAU-1 concentration.....	45
Table 9. Solubility of different gases as a function of CAU-1 concentration.....	45

LIST OF FIGURES

Figure 1. Schematic of comparison between zeolite and imidazole chemical structure [36].....	9
Figure 2. Structure of CAU-1. Green and orange sphere show pores with 10 Å and 5 Å diameters in the framework. (Framework generated in Materials Studio software).....	13
Figure 3. Schematic of reaction for the synthesis of CAU-1	21
Figure 4. Schematic of fabrication of mixed matrix membrane	23
Figure 5. Quantachrome QUADRASORB surface area analyzer	25
Figure 6. Quantachrome automated autosorb iQ for sorption analysis	25
Figure 7. Schematic of custom-made gas separation setup [58].....	27
Figure 8. Constant volume/variable pressure custom-made gas separation/permeation setup	27
Figure 9. Experimental and simulated XRD patterns of CAU-1	29
Figure 10. BET: N ₂ Sorption (Adsorption-Desorption) curve at 77 K.....	31
Figure 11. Sorption isotherms for different gases (CO ₂ , N ₂ , CH ₄) at 298 K	31
Figure 12. CAU-1 crystals morphology at a) Lower magnification, b) Higher magnification	33
Figure 13. Thermogravimetric analysis of synthesized CAU-1 particles.....	34
Figure 14. Cross-sectional images of pure PEI membrane showing a spongy morphology a) lower magnification b) higher magnification.....	36

Figure 15. Cross-sectional images of 5% CAU-1/PEI membrane showing a spongy morphology at a) lower magnification b) higher magnification. CAU-1 embedded particles shown inside white circle.....	37
Figure 16. Cross-sectional image of 10% CAU-1/PEI membrane showing a spongy morphology and uniformly dispersed/embedded CAU-1 particles in PEI walls	38
Figure 17. SEM cross-sectional image of 15% CAU-1/PEI membrane showing a spongy morphology at a) lower magnification b) higher magnification. CAU-1 particle agglomeration shown inside orange circle.....	39
Figure 18. XRD patterns of CAU-1 particles, PEI, 5%, 10% and 15% CAU-1/PEI membranes	40
Figure 19. Schematic of gas molecules passing through symmetric spongy porous membrane.....	42
Figure 20. Diffusion coefficients versus Lennard-Jones diameter	46
Figure 21. Correlation between P_{CO_2} and α (CO ₂ /CH ₄) of Pure PEI (green), 5% CAU-1/PEI MMM (Blue), and 10% CAU-1/PEI MMM (brown) compared to Robeson Upper Bound (Black line) and reported membranes (Red)	48
Figure 22. Correlation between P_{CO_2} and α (CO ₂ /N ₂) of Pure PEI (green), 5% CAU-1/PEI MMM (Blue), and 10% CAU-1/PEI MMM (brown) compared to Robeson Upper Bound (Black line) and reported membranes (Red)	48
Figure 23. Correlation between P_{H_2} and α (H ₂ /N ₂) of Pure PEI (green), 5% CAU-1/PEI MMM (Blue), and 10% CAU-1/PEI MMM (brown) compared to Robeson Upper Bound (Black line) and reported membranes (Red)	49

Figure 24. Correlation between P_{H_2} and α (H₂/CO₂) of Pure PEI (green), 5% CAU-1/PEI MMM (Blue), and 10% CAU-1/PEI MMM (brown) compared to Robeson Upper Bound (Black line) and reported membranes (Red) 49

Figure 25. Correlation between P_{H_2} and α (H₂/CH₄) of Pure PEI (green), 5% CAU-1/PEI MMM (Blue), and 10% CAU-1/PEI MMM (brown) compared to Robeson Upper Bound (Black line) and reported membranes (Red) 50

LIST OF ABBREVIATIONS

PEI	:	Polyetherimide
MOF	:	Metal-organic Framework
ZIF	:	Zeolite Imidazole Framework
MMM	:	Mixed matrix membrane
CAU	:	Christian-Albrechts-Universität
BET	:	Brunauer–Emmett–Teller
GH	:	Green house
SOD	:	Sodalite
DMA	:	Dimethylacetate
TGA	:	Thermogravemetric analysis
XRD	:	X-ray diffraction
SEM	:	Scanning electron microscopy

ABSTRACT

Full Name : Omar Waqas Saadi

Thesis Title : DEVELOPMENT AND PERFORMANCE EVALUATION OF CAU-1 METAL-ORGANIC FRAMEWORK/POLYETHER IMIDE MIXED MATRIX MEMBRANE FOR GAS SEPARATION

Major Field : Materials Science and Engineering

Date of Degree : December, 2017

For last few decades, metal organic framework (MOF)/polymer mixed matrix membranes have shown high potential for gas separation application. Robeson's upper bound correlation states that there is usually a trade-off between permeability and gas selectivity of a polymeric membrane. In the present work, small particles of CAU-1 were synthesized using solvothermal method, processing size distribution of 300-500 nm and BET surface area of $\sim 1149 \text{ m}^2/\text{g}$. These particles were incorporated in polyetherimide (PEI) matrix with different concentrations (5 wt%, 10 wt% and 15 wt% CAU-1) to develop CAU-1/PEI mixed matrix membranes which were tested for gas separation performance. Compared to PEI membrane, the gas separation results for 5% CAU-1 /PEI membrane indicated that the permeability of H_2 , O_2 , N_2 , CO_2 and CH_4 increased from 328, 28.2, 4.28, 91.7 and 5.22 barrer to 633, 52, 10, 193.5 and 10.5 barrer respectively, while the selectivity for H_2/N_2 , H_2/CO_2 , H_2/CH_4 , CO_2/N_2 and CO_2/CH_4 remained unchanged. The permselectivity (a measure of maximum permeability and selectivity) obtained for this mixed matrix membrane is positioned above the Robeson upper bound correlation line for H_2 separation (from O_2 , N_2 and CO_2) and close to the upper bound for CO_2 removal (from N_2 and CH_4) which is desirable for gas separation industry. The permeability of 10% CAU-1/PEI was measured to be 450, 19.2, 2.0, 40, 1.6 for H_2 , O_2 , CO_2 , N_2 and CH_4 with enhanced

selectivity. The 10% CAU-1/PEI membrane showed a higher permselectivity than that of PEI, 5% CAU-1/PEI and 15% CAU-1/PEI prepared in this work, and also higher than PEI based mixed matrix membranes reported in literature for hydrogen separation (H_2/N_2 , H_2/CO_2 , H_2/CH_4).

ملخص الرسالة

الاسم الكامل: عمر وقاص سعدي

عنوان الرسالة: : تطوير و قياس الأداء لاغشية بوليمرات مختلطة من الأطر المعدنية العضوية (CAU-1) و بولي إيثيريميد (PEI) لفصل الغازات .

التخصص: علوم و هندسة المواد

تاريخ الدرجة العلمية: ديسمبر 2017

على مدى العقود القليلة الماضية، أظهرت الأغشية المعدنية العضوية (MOF) \ بوليمر المختلط إمكانات عالية لتطبيق فصل الغاز. تنص علاقة منحني روبيسن الارتباطية العليا على أن هناك عادة مفاضلة بين النفاذية وانتقائية الغاز على الأغشية من أصل بوليمري. في هذا العمل، تم تصنيع جسيمات صغيرة من CAU-1 باستخدام طريقة الاذابة الحرارية، والتي لها توزيع حجم جزيئي من 300-500 نانومتر ومساحة سطح $1149 \text{ m}^2 / \text{g}$ BET. تم دمج جسيمات CAU-1 هذه في مصفوفة بولي إيثيريميد (PEI) بتركيزات مختلفة (5% بالوزن، 10% بالوزن و 15% بالوزن لتطوير أغشية مصفوفة مختلطة CAU-1 / PEI والتي تم اختبارها لأداء فصل الغاز. بالمقارنة مع غشاء PEI، أشارت نتائج فصل الغاز لـ 5% CAU-1 / PEI إلى أن نفاذية H_2 و O_2 و N_2 و CO_2 و CH_4 ارتفعت من 328 و 28.2 و 4.28 و 91.7 و 5.22 إلى 633 و 52 و 10 و 193.5 و 10.5 بارر، على التوالي، في حين أن الانتقائية لـ H_2 / N_2 ، H_2 / CO_2 ، H_2 / CH_4 ، CO_2 / N_2 و $\text{CO}_2 / \text{CO}_2$ ظلت دون تغيير. تم تحديد النفاذية الانتقائي (مقياس النفاذية القسوى والانتقائية) الذي تم الحصول عليه للأغشية المصفوفة المختلطة المصنعة فوق منحني روبيسن في حالات فصل H_2 من غازات O_2 ، N_2 و CO_2 والقريب من الحد الأعلى لإزالة CO_2 من غازات N_2 و CH_4 وهو أمر مرغوب فيه لصناعة فصل الغاز. تم قياس نفاذية 10% CAU-1 / PEI لتكون 450 و 19.2 و 2.0 و 40 و 1.6 لـ H_2 و O_2 و CO_2 و N_2 و CH_4 مع انتقائية محسنة. أظهر غشاء الـ 10% CAU-1 / PEI قدرة انتقائية أعلى من PEI و 5% CAU-1 / PEI و 15% CAU-1 / PEI التي تم إعدادها في هذا العمل، وهي أعلى أيضاً من أغشية المصفوفة المختلطة PEI المسجلة في الأدبيات لفصل الهيدروجين، كما في حالات H_2 / CO_2 ، H_2 / N_2 ، H_2 / CH_4 .

CHAPTER 1

INTRODUCTION

Global warming is becoming a crucial environmental concern. 'Our ecosystem is warming' has been confirmed by many scientific proofs. [1][2] These proofs come from many indicators in our ecosystem which include changes in atmospheric vapor pressure, sea level, atmospheric temperature, and glaciers. According to scientists, there is a 90% certainty that greenhouse gases are involved in the global warming of our system with some other human activities also. [3] One of the components of greenhouse gas is carbon dioxide which plays a major part in the global warming of our ecosystem. Carbon dioxide is continuously increasing in the atmosphere due to the burning of fuels and the vegetation is only able to absorb half of this produced carbon dioxide. [4]

The unchecked release of carbon dioxide can result in the shutdown of ocean circulation which would be a major change for the planet and one can only imagine the after effects. [5] Some abrupt and large-scale changes such as landslide, increase in sea level and ocean acidification may be caused by the increase of CO₂ amount in the troposphere; as the CO₂ remnants in the air for an extended period of time. Waters in the oceans have already begun to acidify by the increase of carbon dioxide in the atmosphere. [6]

Therefore it is important to control the amount of carbon dioxide emissions to the environment to stabilize universal temperature. According to a study, the emissions of CO₂ should be decreased by more than 80%. But CO₂ will still be in our environment

for a very long time before it decreases to a minimum level and the result would be high temperatures due to the presence of CO₂. [7]

1.1 Flue gas

Flue gas comprises N₂, CO₂, O₂ and water vapors. Small quantities of oxides of sulfur, nitrogen, and carbon are also present in the flue gas. Flue gas is generated during combustion and it has more than 60% nitrogen in it. Usually, they are produced from power plants and exits through a chimney, hence the name flue. Burning constituents determine the composition of flue gas. Gas separation is getting much attention to remove carbon dioxide from the flue gases, so a high-quality carbon dioxide gas can be provided to food and oil industries.

1.2 Natural gas

Global natural gas consumption is around 3.1 trillion cubic meters [8] and overwhelms other industrial applications of gas separation. The composition of natural gas varies depending upon the location of reservoirs. But it majorly comprises of methane (30-90%), containing also heavy hydrocarbons along with CO₂, N₂, H₂S and He. The pipelines used to transfer raw natural gas have certain specifications which need to be met prior the transfer by processing natural gas otherwise the contents of natural gas, for example, CO₂ being acidic in nature when combined with water vapors may damage the pipeline. The natural gas processing costs billions of dollars per annum to meet the specified objectives. Therefore membrane technology is a cost-effective as well as an efficient mode to replace or at least minimize the use of other expensive processing techniques.

1.3 Responses to global warming

There are some possible responses to global warming. These responses include:

1.3.1 Mitigation

Mitigation refers to the actions taken to reduce global warming by the reduction of mainly CO₂ and some GH gases. Production of CO₂ and greenhouse gases in the environment can be reduced by the use of solar energy, nuclear energy, wind and tidal energy instead of burning of fossil fuel which generates the greenhouse gases. Carbon capture and storage can also reduce the emissions of carbon dioxide to the environment by significant amounts. [9]

1.3.2 Adaptation

Adaptation is the type of response which aims to decrease the effect of global warming and climate changes on social and biological systems. [10] Adaptation is still a necessity even if the discharges of greenhouse gases were to be reduced since the effect of these gases remains in the environment for a long time. [11] The capacity of humans to acclimate to certain changes is known as adaptive capacity and it not evenly scattered all over the world. It is very less in developing countries and therefore adaptation is very necessary in those countries. [12]

1.2.3 Climate Engineering

Climate engineering refers to the changes in climate in order to limit or reduce the adverse effects. Two types of cases present themselves in climate engineering; CO₂ elimination and solar radiation management. CO₂ elimination refers to the removal of CO₂ from the GH gas whereas solar radiation management deals with the absorption of solar radiations by the earth to remove the adverse effects. [13]

CHAPTER 2

LITERATURE REVIEW

To reduce global warming, generation of greenhouse gases should be stopped or at least there should be a limit. As discussed earlier one way to reduce global warming is the carbon dioxide separation or storage. Extensive research is being done on gas separation to reduce the global warming. Gas separation is one of the methods to separate gases resulting in either a pure single product or several products. There are several techniques for gas separation. Some of these techniques are mentioned below.

2.1 Swing adsorption techniques

2.1.1 Pressure swing adsorption

In this technique a gas is first pressurized around adsorbent to capture certain components from the gas selectively while leaving others and then depressurized to produce the captured or adsorbed components.

2.1.2 Vacuum swing adsorption

This technique works on the same principle as that of pressure swing adsorption. The only difference is that it operates between atmospheric pressure and vacuum pressures. The two techniques can be combined to get vacuum pressure swing adsorption.

2.1.3 Temperature swing adsorption

The technique of temperature swing adsorption is the same as that of the above-mentioned techniques with the difference of use of temperature instead of pressure to adsorb and desorb certain components from a gas.

2.2 Cryogenic distillation

This technique is used for large volumes of gases because of the high energy consumption and cost and produce high purity gas components from atmospheric air. Mostly nitrogen and oxygen are separated from the other gases in the atmospheric air. The principle is to liquefy the air by cooling it and then heating to boiling temperature of different gases to remove them selectively. [14]

2.3 Membrane gas separation

Membrane gas separation technologies are not widely used because they are not well developed. Gases can be separated using a membrane which is synthesized from polymers like polyimide, polyamide, polysulfone, polyethylene or ceramics or a combination of both. Two varieties of membranes exist; non-porous and porous.

2.3.1 Non-Porous membranes

Non-porous membranes usually consist of polymers and are highly dense membranes. Non-porous membranes should be very thin to get high selectivity. The rate of transport of gases through these membranes depends on the temperature according to Arrhenius equation. [15] The small molecules of gases entering pass through the polymer chain gaps as polymer molecules have thermal vibrations. Mostly the separation is based on the molecular size of the component.

2.3.2 Porous membranes

Larger voids are present in porous membranes which are interconnected to one another and allow the molecules with greater sizes to pass through the membrane. Since the pore size is larger in porous membranes they usually give poor selectivity. Gas flux is higher in porous membranes than non-porous membranes by an order of 4 and it is inversely proportional to the molecular mass of gases passing through the membrane.

2.4 Membrane separation properties

2.4.1 Permeability

Permeability is the potential of a solid or membrane to permit the molecules of gas or liquid to pass through it. Permeability (P) is a product of sorption coefficient (K) and diffusion coefficient (D). It can be mathematically expressed as

$$P = K \cdot D \quad (1)$$

Sorption coefficient deals with the amount of gas that has been adsorbed in the membrane. The diffusion coefficient, as the name suggests, refers to the diffusion of molecules across the film. It describes the surrounding's effect on gas molecules' motion when they are being diffused.

Permeation of gas when there are no pores present in material refers to diffusion flow such as polymers permeability. Permeation of gas across a porous body, having pores whose diameter is lesser than the mean free path of molecules (at 133.322 N/m² of pressure) is termed as a molecular effusion.

The laminar flow of a gas occurs in a porous structure when the diameter of these pores is very large than mean free path.

The membrane permeance P is defined as:

$$P = \frac{J}{A \cdot \Delta p} \quad (2)$$

Where J is the permeate rate given in mol/sec, A is the area of the component or sample, Δp stands for pressure difference.

2.4.2 Permeation flux

The amount of gas passing through a unit area of membrane at unit time is known as permeation flux. Temperature and pressure affect the amount of gas passing through a membrane. Usually, the calculation is done under standard conditions of 0° Celsius and 1 atm pressure.

2.4.3 Selectivity (Separation factor)

The capacity of a membrane to separate two different gases is known as selectivity. It is expressed as the ratio of permeability (P) of two gases:

$$\alpha = P_A/P_B \quad (3)$$

Where A and B designate two different gases.

2.5 Metal-Organic Framework membranes

Metal-organic frameworks (MOFs) involve an organic part and an inorganic part which are linked to each other through chemical bonds. Inorganic parts are metals ions or clusters. Inorganic metal ions and organic molecules combine to produce a structure which is porous in nature. The organic part of the MOFs is also called struts, linkers or ligands.

Each MOF material has a different pore aperture size. MOFs allow the gas molecules with smaller sizes than their pore aperture sizes to pass through. But sometimes larger molecules can also pass through at an increased pressure. When pressure is increased it results in the opening of 6 membered rings in SOD structures as there is thermal rotation present in linkers. This phenomenon is called Gate opening mechanism.

Zeolite imidazolate framework, also known as ZIF, is a subclass of metal-organic framework. ZIFs are the hybrid structure of an inorganic part (transition metal ions

tetrahedra) and organic part (imidazolate ligands). Organic imidazolate ligands act as linkers between two consecutive metal ions [27-29]. ZIFs have similar topology to zeolites and are very porous. ZIFs' thin membranes find applications in chemical sensors, gas separation, electrical devices, and optics [30,31]. The organic linkers present in ZIFs aid in tunability of the structure which is advantageous for chemical sensors [21]. A lot of research is being carried on MOF membranes for gas separation. Being thermally and chemically stable with a microporous structure, ZIFs have found much attraction in industries for gas separation [22]. Zeolitic Imidazolate framework membranes first appeared in the late 2000s. It was discovered that zeolite had Si-O-Si of 145° which was same as that of M-Im-M links (where M can be any transition metal with tetra coordinate and tetrahedral structure)(Figure 1) [23]. Thus, theoretically it should be possible to prepare any kind of zeolitic imidazolate framework. This coincident behavior has resulted in over 100 different ZIF structures [23]. All the ZIFs that have been synthesized until now have been reported to have very porous structures with different aperture sizes. Some ZIF membranes prepared and reported until now are ZIF-7[24], [25], ZIF-8[26], [27], ZIF-22[28], ZIF-69[29], ZIF-78[30], ZIF-90[31], [32], ZIF-93[33], ZIF-95[34], and ZIF-100[35].

Usually, ceramic substrates are used for film fabrication. It has also been reported that ZIFs films can be fabricated on flexible polymer supports like nylon which provides good flexibility to the structure. [37] The nucleation of metal-organic frameworks on ceramic substrates is very difficult. According to a study, the nucleation density of these crystals is very low when a ceramic support is being used. [38] Chemical modifications of ceramic support surfaces can allow preparing MOFs membranes with better nucleation and growth of crystals.

There are a lot of techniques for the preparation of metal-organic framework-based membranes. Some of these are:

- Solvothermal growth with modification of support surface
 - ✓ with organosilane molecules [39], [40], [41], [42] or
 - ✓ organic ligands [43]
- Solvothermal growth without modification of support surface
- Spin coating [44]
- Layer-by-layer growth [45]
- Microwave-induced thermal deposition [46]
- Electrochemical synthesis [47]
- Solvent evaporation [46]
- Secondary growth [38]

2.6 Mixed-matrix membranes

Polymeric membranes manufactured from organic materials have been used commercially for CO₂ removal since the 1980s due to their affinity towards CO₂. [8] But their efficiency is still questionable due to a trade-off between permeability and selectivity as stated by Robeson [48]. Polymeric membranes are non-porous having

very low permeability or flux. Therefore, for the past couple of decades a lot of research is being conducted on silica, carbon or zeolite-based inorganic membranes, however, these membranes have their own drawbacks like defective structures, a high fragility and low packing density which makes it hard to commercialize these membranes in industry. This resulted in the idea of mixed matrix membranes.

Mixed matrix membranes are composite membranes with metal-organic frameworks as filler material embedded in the polymer matrix and combine the good properties of metal-organic frameworks and polymers. Thus, they are supposed to provide better gas separation results since the introduction of filler particles can enhance the flux and can have certain affinity towards some of the gas molecules. Fillers which are commonly used in the fabrication of mixed-matrix membranes can be porous (for example MOFs, zeolites and carbon-based materials like activated carbon, carbon nanotubes), and non-porous (like silica, titania). All these mentioned materials, except MOFs, are inorganic and show poor physical interaction with polymeric membranes which are organic in nature. Hence it is very difficult to prepare a uniform mixed matrix membrane having good permselectivity using inorganic particles [49].

Incorporating inorganic particles in polymeric matrix leads to particle agglomeration and generation of interfacial defects due to poor interaction between the two resulting in a decrease in selectivity [50]. A lot of studies has been done on post modification and functionalization of inorganic particles to reduce the above-mentioned defects. However, the presence of organic linkers in metal-organic frameworks makes them suitable to use in mixed matrix membranes even without modification, making them the best material to use in mixed matrix membranes. It has been reported in some of the studies that using metal-organic frameworks without post-synthetic modification in mixed matrix membranes results in improvement of permselectivity because of the

mitigation of nonselective interfacial voids. One of the studies of this type was carried out using MOF-5 in Matrimid matrix to enhance the gas permeability with no effect on the gas selectivity of CO₂/CH₄ [50].

Choosing a proper combination of metal-organic frameworks and polymer is very crucial for the preparation of a defect-free mixed matrix membrane. Here we choose CAU-1 (CAU-1-NH₂) metal-organic framework as filler material and polyetherimide as a matrix. Amino groups present in CAU-1 could form a significant amount of hydrogen bonds with methyl groups and oxygen present in polyetherimide, resulting in an interfacial void-free mixed matrix membrane. Ahnfeldt et al. [51] reported the synthesis of a CAU-1 metal-organic framework for the first time in 2009. CAU-1 is aluminum-based MOF with a tetragonal crystal structure and is stable till 300 °C. CAU-1 when heated at 100 °C shows a weight loss of around 6% which is attributed to the evaporation of water molecules in the structure. The Langmuir surface area for CAU-1 was found to be 1700 m²/g with a pore volume of 0.52 cm³/g [51]. The structure of CAU-1 exhibits two pores with diameter of 10 Å and 5 Å depending on the arrangement of wheel-shaped 8-ring building unit. But these pores are only accessible through small pore windows of 3-4 Å. The wheel-shaped 8-ring building unit is formed from {AlO₆} polyhedra connected to each other at corners and edges through hydroxide and methoxide groups. Each Al⁺³ is connected coordinatively to 3 carboxylate oxygen atoms, 1 hydroxide, and 2 methoxide ions. The wheel-shaped 8-ring building unit is linked to 12 other wheel-shaped units through aminoterephthalate ions; 4 of which lie in the same plane, 4 above and 4 below it. (Figure 2)

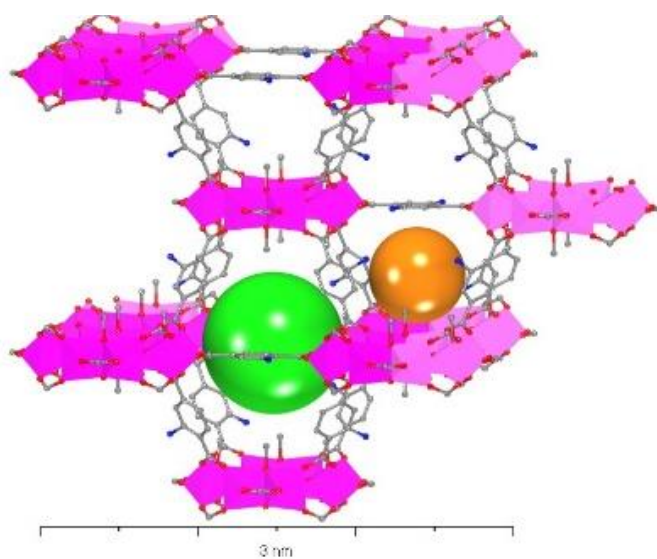


Figure 2. Structure of CAU-1. Green and orange sphere show pores with 10 Å and 5 Å diameters in the framework. (Framework generated in Materials Studio software)

One patent [50] compared gas permeability performance of IRMOF-1/matrimid mixed matrix membrane with that of IRMOF-1/polyetherimide mixed matrix membrane for CO₂ removal from natural gas and found an increase in permeability of CO₂ through IRMOF-1/PEI MMM by the order of 2-3 times compared to the IRMOF-1/Matrimid membrane. They found the CO₂/CH₄ selectivity in both the membranes to be same and they owe this selectivity to the glassy structure of polymers.

García et al. [52] studied the effect of particle size and loading of activated carbon (AC) on the mechanical properties of AC/PEI mixed matrix membrane. It was found that the mixed matrix membrane lost its flexibility, Young's modulus and became rigid as the particle concentration was increased. Gas separation permselectivity performance of AC/PEI mixed matrix membrane was also evaluated. Increase in the particle size incorporated in mixed matrix membrane resulted in poor adhesion between the polymer matrix and the particles producing interfacial voids which cost the membrane its selectivity. An increase in gas selectivity was found for 10% AC/ PEI mixed matrix membrane compared to the pure PEI membrane for different pairs of gases; H₂/CH₄, H₂/CO₂, O₂/N₂. Increase in further concentration of AC particles decreased mechanical properties of mixed matrix membranes rendering them useless for gas separation analysis as shown in Table 1. Selectivity results are shown in Table 3.

Table 1. Mechanical properties of AC/PEI MMMs [52]

Membrane	σ (MPa)	ϵ (%)	E (GPa)	Toughness (kJ/m ³)
0 % AC/PEI	67.85	10.33	1.221	4620.3
2 % AC/PEI	95.60	9.00	1.329	4223.9
10 % AC/PEI	34.19	6.80	0.869	891.8
20 % AC/PEI	14.91	6.60	0.614	532.5

Another study [53] reported gas separation performance of ZIF-90/PEI mixed matrix membrane. Solvothermally produced ZIF-90 crystals have an average size of around 2 μm . In this study, ZIF-90 crystal growth was inhibited by adding a non-solvent in the reaction solution at room temperature. This way nucleation was preferred instead of crystal growth and crystal size was obtained with an average of 0.8 μm . Thermogravimetric analysis of these two types of crystals showed that ZIF-90 crystals with a smaller size (0.8 μm) were stable up to 290 $^{\circ}\text{C}$ as compared to larger ZIF-90 crystals (2 μm) which were stable up to 250 $^{\circ}\text{C}$. Gas selectivity for CO_2/CH_4 remained unchanged of ZIF-90/PEI membrane but CO_2 permeability was increased as compared to pure PEI membrane from 1.4 barrer to 2.9 barrer. They attribute this trend to Maxwell's model that when filler particles have high permeability than matrix the selectivity will always remain the same but there will be an increase in permeability of mixed matrix membrane. We believe the interfacial voids can be avoided by using small particles as fillers in mixed matrix membranes.

A lot of researchers have studied dense membranes, whether polymeric or mixed matrix, for gas separations. A very few have studied asymmetric hollow fibers. Dai et al. [54] report permselectivity of 13% ZIF-8/PEI asymmetric hollow fiber membranes for the CO_2/N_2 pair and found an increase in CO_2 permeation and CO_2/N_2 selectivity by 85% and 20% compared with that of the pure dense membrane and pure hollow fiber. The reason behind this could be the polymeric chain orientation in hollow fiber mixed matrix membrane since the membrane was fabricated by spinning out viscous polymeric solution containing ZIF-8 particles through a narrow orifice.

Chen et al [52] studied gas separation performance of MIL-53(Al) and NH_2 -MIL-53(Al) incorporated in Matrimid (Polyimide) and Ultem (PEI) matrix for a comparison for a CO_2/CH_4 pair with different concentrations of fillers in mixed matrix membranes.

MIL-53(Al) and NH₂-MIL-53(Al) were synthesized with a particle size in the range 100-150 nm with BET surface area of MIL-53 (1440 m²/g) higher than that of NH₂-MIL-53 (840 m²/g). But an interesting development was found with TGA of these two particles. Amino based MIL-53 was found to be stable at a higher temperature (400 °C) than MIL-53 (200 °C). NH₂-MIL-53 based mixed matrix membranes showed 1.5 times CO₂ permeability than MIL-53 based MMMs. Furthermore, it was found that polyetherimide based mixed matrix membranes have a higher selectivity for CO₂/CH₄ pair than polyimide-based mixed matrix membranes as can be seen in Table 2. Matrimid and Ultem are commercial names for polyimide and polyetherimide respectively.

Table 2. Gas permeability, ideal selectivity of MIL53 and NH2-MIL53 with Matrimid and Ultem mixed matrix membranes [52]

Membranes	Permeability CO ₂ (Barrer)	Permeability CH ₄ (Barrer)	α (CO ₂ /CH ₄)
Matrimid	6.2	0.2	31
15%-MIL53/PI	6.7	0.71	9.4
15%-MIL53-NH ₂ /PI	9.2	4.4	2.1
Ultem	1.46	0.037	39.5
15%-MIL53/PEI	1.77	0.041	43.1
15%-MIL53-NH ₂ /PEI	3.0	0.083	36.2

In another article, Duan and group [52] incorporated HKUST-1 in the polyetherimide matrix and studied selectivities for CO₂/N₂ and CO₂/N₂ of the mixed matrix membrane.

An increase in permeability of gases was found in mixed matrix membranes compared to pure polyetherimide membrane while the selectivities for pure membrane and mixed matrix membrane remained unchanged. The increase in permeability was attributed to the increase in diffusivity of the mixed matrix-matrix membrane due to the addition of HKUST-1 particles. CO₂ permeability for mixed matrix membrane was increased by 2.6 times.

Table 3. Permeability P (Barrer) and selectivity α of different mixed matrix membranes from the literature

Membranes (wt%)	Filler	P_{H_2}	P_{O_2}	P_{N_2}	P_{CO_2}	P_{CH_4}	$\alpha(\frac{H_2}{O_2})$	$\alpha(\frac{H_2}{N_2})$	$\alpha(\frac{H_2}{CO_2})$	$\alpha(\frac{H_2}{CH_4})$	$\alpha(\frac{O_2}{N_2})$	$\alpha(\frac{CO_2}{N_2})$	$\alpha(\frac{CO_2}{CH_4})$
PEI [52]	10% AC	13.51	1.073	0.132	2.087	0.050	12.59	102.35	6.47	270.2	8.13	15.81	41.74
Ultem[53]	15% ZIF-90	-	-	-	2.9	0.074	-	-	-	-	-	-	39
Ultem[54]	13% ZIF-8	-	-	-	26GPU	-	-	-	-	-	-	36	-
PEI[55]	15% MIL-53	-	-	-	1.77	0.041	-	-	-	-	-	-	43.1
PEI[55]	15 % NH ₂ -MIL-53	-	-	-	3.00	0.083	-	-	-	-	-	-	36.2
Ultem[56]	35% HKUST-1	-	-	-	4.13	0.1215	-	-	-	-	-	-	33.99
Ultem [57]	25% T-MOF-5	25.2	-	0.14	3.00	0.12	-	180	8.45	208.02	-	21.42	22.57
PEI [58]	5% nZIF-7	207.0	15.9	3.8	64.7	5.0	13.0	53.9	3.2	41.8	4.2	16.8	13.1
PEI [59]	25% cMOF-5	28.32	-	0.19	5.39	0.23	-	149.05	5.25	123.89	-	28.36	23.43
PEI [58]	PSM-nZIF-7	2020.9	272.9	182.6	245.9	107.9	7.4	11.1	8.2	18.7	1.5	1.3	2.3
PEI [60]	20% IRMOF-1	16.9	-	-	2.97	0.113	-	-	5.69	149.3	-	-	26.3

2.7 Thesis Aim/Objectives

The aim of the present study is to develop a metal-organic framework (MOF) based membrane for gas separation applications. To achieve this aim, the following objectives have been addressed:

- Synthesis of CAU-1 MOF particles using solvothermal method.
- Characterization of CAU-1 particles using
 - XRD for confirmation of MOF crystal formation
 - BET for surface area
 - SEM for morphology and particle size
 - TGA for thermal stability
 - CO₂, N₂, CH₄ adsorption isotherms for uptake volume
- Fabrication of polyetherimide (PEI) membrane.
 - Study gas separation performance of pure PEI membrane for different gases (H₂, O₂, N₂, CO₂, CH₄)
- Development and characterization of CAU-1/PEI mixed matrix membrane with different volume fractions
- Evaluation of the gas separation performance of the developed mixed matrix membranes

CHAPTER 3

EXPERIMENTAL WORK

3.1 Synthesis of CAU-1

All chemicals and reagents of analytical grade were commercially available and used as received. The typical synthesis procedure of CAU-1 (metal organic framework, MOF) is obtained from the reference [51]. A mixture of $\text{AlCl}_3 \cdot 6\text{H}_2\text{O}$ (2.967 g, 12.3 mmol) and $\text{H}_2\text{N}-\text{H}_2\text{BDC}$ (0.746 g, 4.1 mmol) was suspended in methanol (30 ml) and heated at 125 °C for 5 h. Then, the obtained CAU-1 powder was heated at 120 °C for 24 hours (Figure 3). The yield of CAU-1 was around 200 mg using an autoclave of volume 20 ml. Two autoclaves were used at the same time to prepare a total of 400 mg of CAU-1 particles. The CAU-1 framework shown in figure 3 was drawn using Materials Studio software.

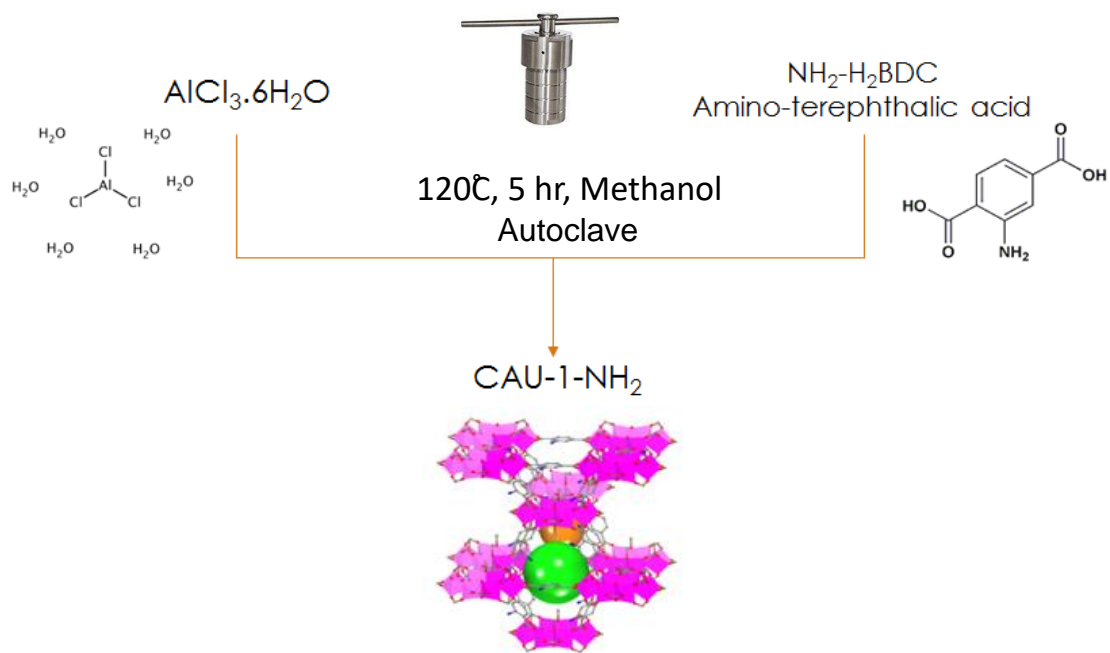


Figure 3. Schematic of reaction for the synthesis of CAU-1

3.2 Preparation of CAU-1/PEI membrane

There are mainly two steps for the preparation of mixed matrix membranes (MMMs). The first step is to disperse the filler in the solvent with an ultrasonic bath. The second step is to add polymer. We have prepared 5wt%, 10wt%, and 15wt% based MMMs (Table 4). In all cases, the quantity of dimethylacetamide (DMAC) was kept 2.4 ml. Typically, for example, for 15 wt.% concentration, 0.112g CAU-1 was sonicated in 2.4 ml dimethylacetamide (DMAC) in an ultrasonic bath for 2 hours and 0.63g Polyetherimide (PEI) was carefully dissolved at 45 C for 24 hours on magnetic stirrer under stirring. Before the casting, different intervals of sonication and stirring take place to ensure a well dispersion (Figure 4). Subsequently, the membranes are cast on a flat glass surface and then left overnight for evaporation of solvent at room temperature. Once dried, the membranes are washed 4 times with methanol and then dried to remove the remaining solvent. All the membranes were treated with 30 wt.% PDMS/n-hexane solution by dipping them in solution for 10 seconds and leaving in open air to dry. This treatment was carried out to fill up any surface cracks.

Table 4. Concentration of CAU-1 particles and PEI used to synthesise different membranes

Membrane	CAU-1 wt. (g)	PEI wt (g)	DMA (ml)
Pure PEI	0	0.63	2.4
5% CAU-1/PEI	0.033		
10% CAU-1/PEI	0.07		
15% CAU-1/PEI	0.112		

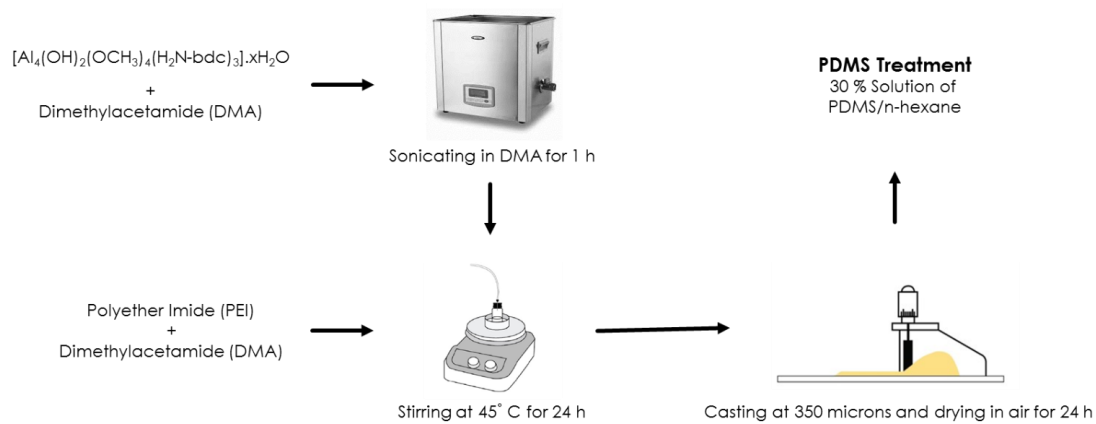


Figure 4. Schematic of fabrication of mixed matrix membrane

3.3 Characterization

CAU-1 crystals and CAU-1/PEI membranes were characterized for the crystal structure using Rigaku benchtop miniflex II XRD system with $\text{CuK}\alpha$ radiation at 30 kV and $3^\circ/\text{sec}$ scan speed in 2θ range of $5\text{-}35^\circ$. Nitrogen adsorption measurements were carried out to measure the BET total surface area and micropore volume of CAU-1 powder (~100 mg) using Quantachrome QUADRASORB (*evo*) Automated Surface Area and Pore Analyzer (Figure 5). Sorption Isotherms were obtained for N_2 , CO_2 and CH_4 to calculate the uptake of each gas (uptake is defined as the adsorption of a given gas molecules on to particles surface and/or pores) by the CAU-1 particles (~100 mg) using Quantachrome autosorb iQ automated gas sorption analyzer (Figure 6). In order to obtain reliable results, samples were evacuated first in a degasser using QUADRASORB system to remove any gas molecules or methanol before BET surface area analysis and sorption analysis.

SEM analysis was carried out to determine the crystal size and to characterize the morphology of the dispersed phase, using a TESCAN company LYRA 3 model operated at 15–20 kV. The weight loss curves (TGA) were recorded, using a Mettler TGA 2 (SF), from 100 to 1000 °C at a heating rate of 10 °C/min under air.



Figure 5. Quantachrome QUADRASORB surface area analyzer



Figure 6. Quantachrome automated autosorb iQ for sorption analysis

3.4 Gas separation analysis

The gas separation measurement was carried out using a custom-made equipment, which is the same as that used by Bassem et al. [58], for H₂, O₂, N₂, CO₂, CH₄. Working of this equipment requires the aid of a schematic to explain in detail how gas permeation system works. As shown in figure 7, the system has pressure regulators, for example, A, an upstream gas chamber B, a downstream gas chamber F, cell D containing membrane, and vacuum pumps H and I connected to each gas chamber. Both of the gas chambers and membrane are evacuated first using valves A2 and A3. Then a given gas, for instance H₂, is filled in upstream gas chamber B at a pressure of 1560 torr and room temperature. The gas is allowed to pass through the membrane, kept in cell D, from upstream gas chamber to downstream gas chamber. The change in the pressure of both gas chambers is measured constantly with the help of transducers and saved in the computer against time. This technique is known as constant volume/ variable pressure technique. The permeability P can be calculated using the following equation:

$$P = 10^{10} \left(\frac{dp_d^{SS}}{dt} - \frac{dp_d^{LR}}{dt} \right) \frac{V_d l}{(p_{up} - p_d)} ART \quad (4)$$

Where P is the permeability coefficient in Barrer ($10^{-10} \text{ cm}^3(\text{STP}) \text{ cm}/(\text{cm}^2 \text{ s cmHg})$), $\frac{dp_d^{SS}}{dt}$ is the downstream pressure rise (cmHg/s) at the steady state, $\frac{dp_d^{LR}}{dt}$ is the downstream “leak rate” (cmHg/s), V_d is the downstream volume (cm^3), l is the membrane thickness (cm), p_{up} is the upstream pressure (cmHg), p_d is the downstream pressure (cmHg), A is the membrane area (cm^2), R is the gas constant [$0.278 \text{ cm}^3 \text{ cmHg}/(\text{cm}^3(\text{STP}) \text{ K})$], and T is the temperature at measurement (K). [58]

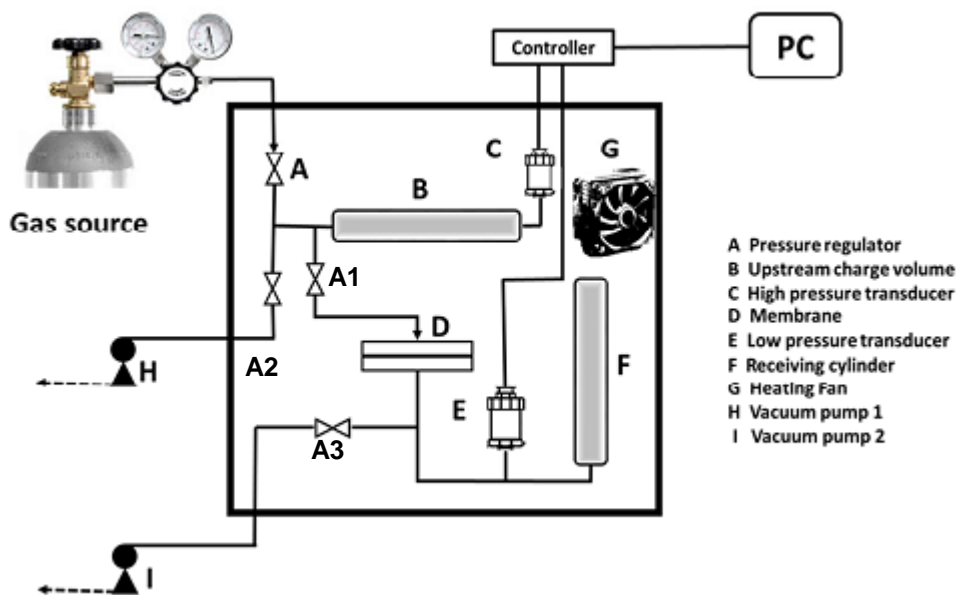


Figure 7. Schematic of custom-made gas separation setup [58]

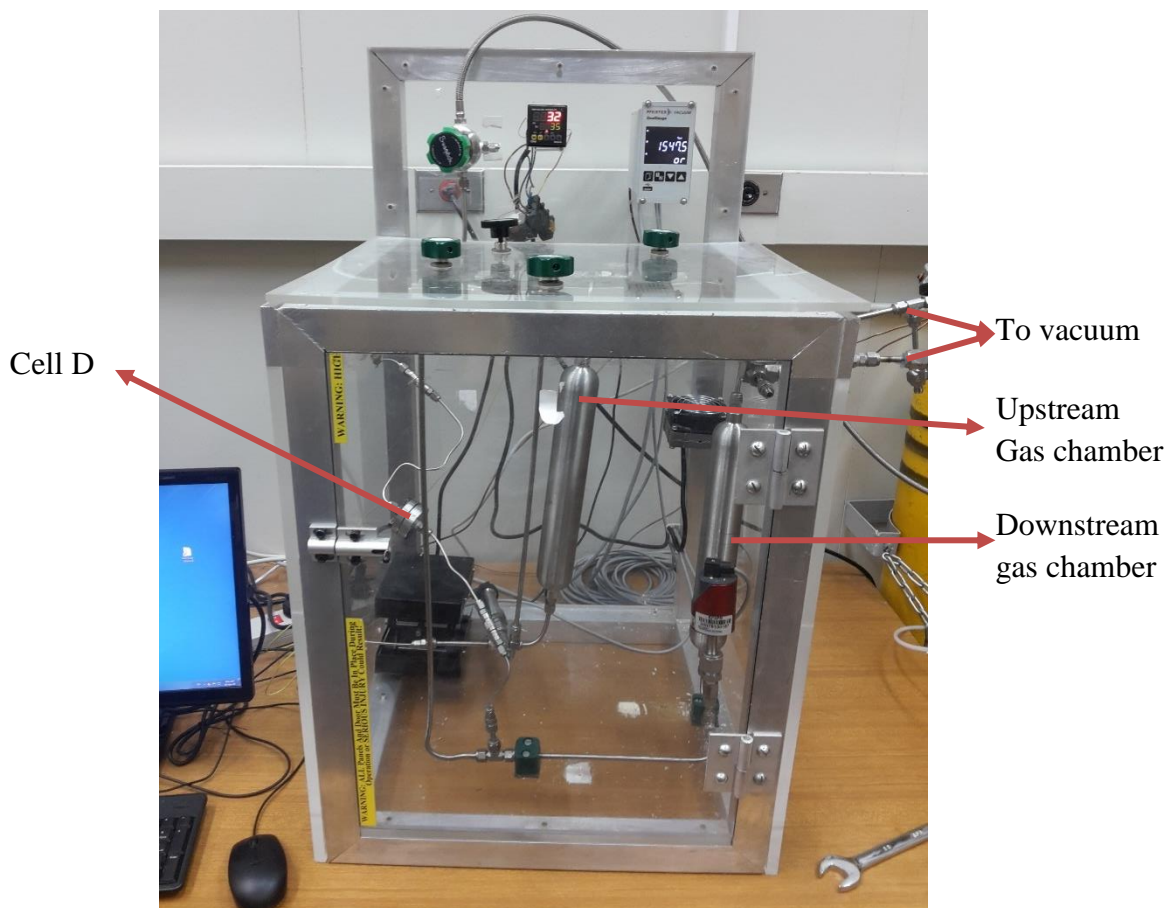


Figure 8. Constant volume/variable pressure custom-made gas separation/permeation setup

CHAPTER 4

RESULTS AND DISCUSSION

Many samples were prepared in order to optimize the parameters for synthesis of CAU-1 and fabrication of polyetherimide (PEI) and mixed matrix membranes.

4.1 CAU-1 Characterization

4.1.1 Powder X-ray Diffraction (XRD)

The synthesis of CAU-1 crystals was confirmed by XRD characterization. Figure 9 contains the XRD patterns of synthesized and simulated CAU-1. Simulated XRD pattern was obtained by running “.cif file” of CAU-1 in Material Studio software. CIF file contains unit cell structure of the CAU-1. It can be seen clearly from Figure 9 that both these patterns (experimental/synthesized and simulated) match well, which confirms the CAU-1 structure and phase purity for the synthesized particles. XRD was performed for every batch prepared.

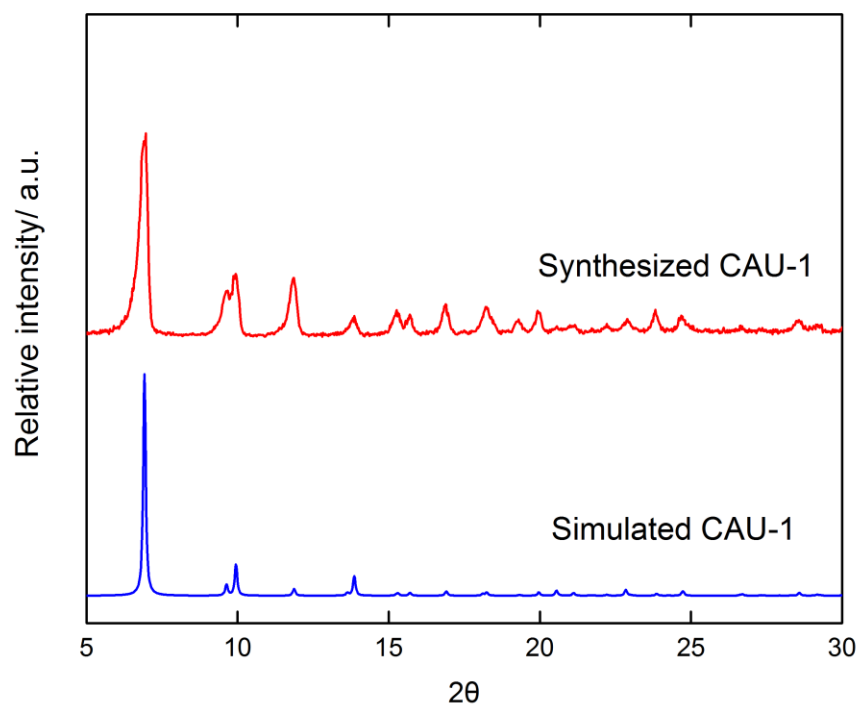


Figure 9. Experimental and simulated XRD patterns of CAU-1

4.1.2 BET analysis

Nitrogen sorption isotherms were used to calculate the BET specific surface area of CAU-1 at 77 K. Figure 10 displays the measured adsorption and desorption points in volume uptake vs partial pressure. The surface area was calculated to be 1149 m²/g, similar to that reported in literature [51]. Furthermore, it can be observed from the adsorption and desorption curves that there is no hysteresis, which means adsorption and desorption of N₂ at 77 K occur smoothly, this is an indication of physisorption.

4.1.3 Sorption analysis

Sorption isotherms were evaluated for CO₂, N₂ and CH₄ to calculate the uptake of each gas in CAU-1 particles. The isotherms are shown in Figure 11. We can deduce from this figure that the uptake for the considered gases in CAU-1 is according to the following order:

$$\text{CO}_2 > \text{CH}_4 > \text{N}_2$$

This indicates that our MOF shows higher adsorption for CO₂ than CH₄ and N₂, revealing that CAU-1 has a good potential to selectively remove CO₂ from N₂ and CH₄ gas mixtures. No hysteresis is observed in any isotherm indicating that CAU-1 material is suitable for gas separation.

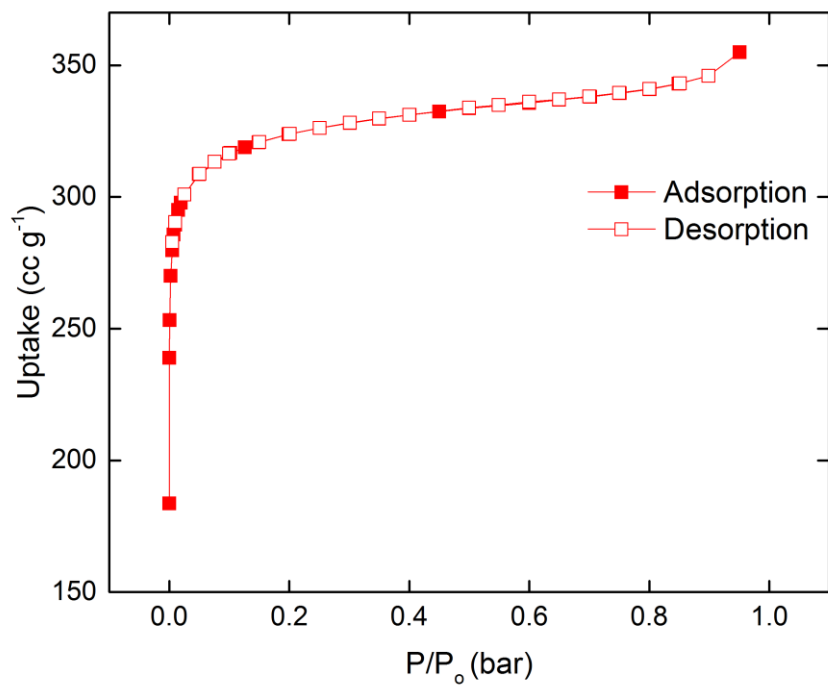


Figure 10. BET: N₂ Sorption (Adsorption-Desorption) curve at 77 K

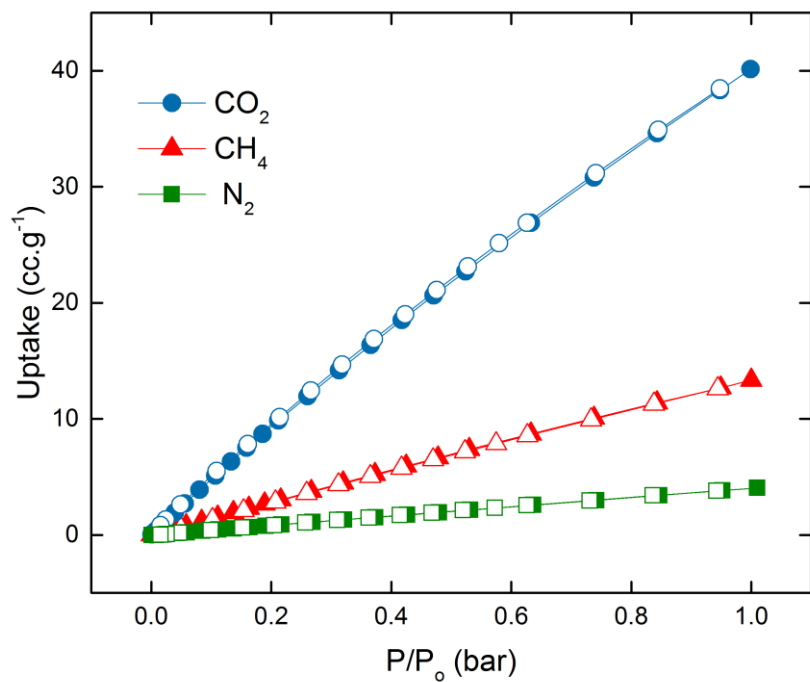


Figure 11. Sorption isotherms for different gases (CO₂, N₂, CH₄) at 298 K

4.1.4 Scanning electron microscopy (SEM)

Figure 12 shows SEM images of CAU-1 crystals taken at 20 kV. A uniform morphology can be seen throughout the crystals with a crystal size distribution of 300-500 nm. The smaller crystal size helps in wetting of crystals by polymeric phase which leads to void free mixed matrix membrane. However, smaller crystals tend to form agglomerates which degrade the mechanical as well as gas separation properties of mixed matrix membranes, but this can be overcome using bath sonication for long time (more than 1 hour).

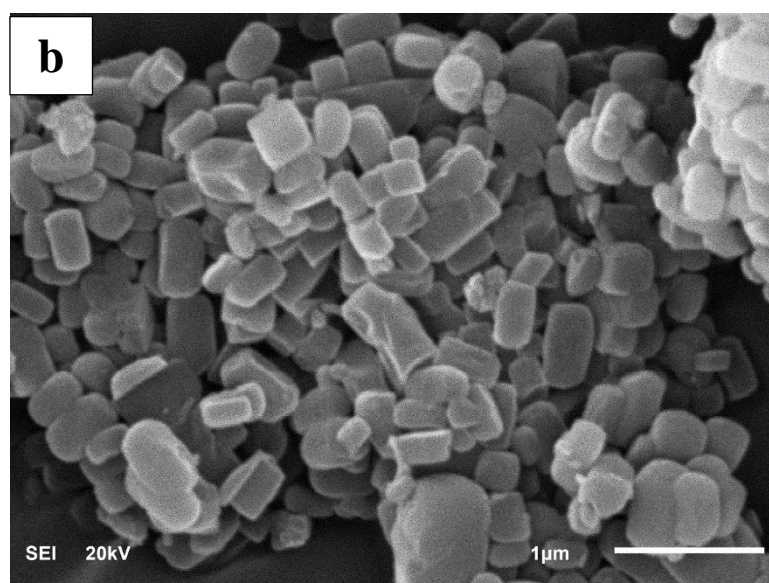
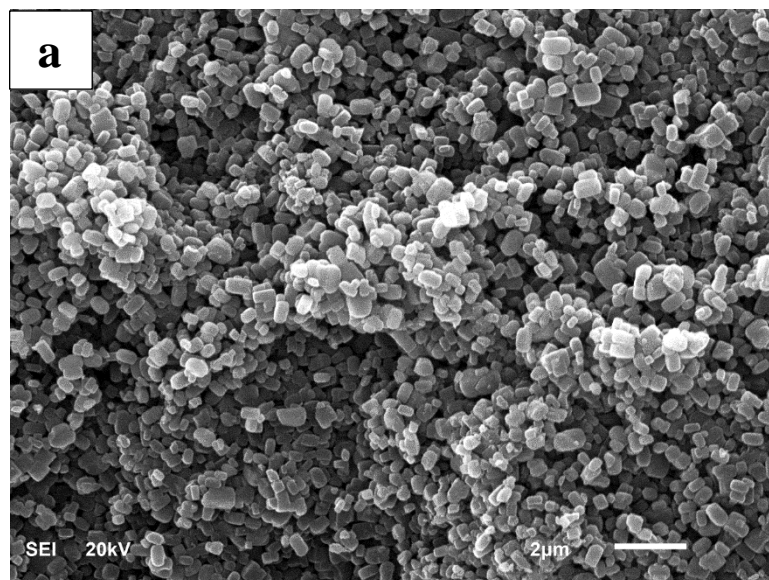


Figure 12. CAU-1 crystals morphology at a) Lower magnification, b) Higher magnification

4.1.5 Thermogravimetric analysis (TGA)

TGA performed up to 660°C for CAU-1 particles is shown in Figure 13. The thermal stability of CAU-1 is in accordance with the literature [51]. The first drop in weight loss in the curve occurs at around 45°C corresponding to around 6-8% weight loss. A single unit cell of CAU-1 contains three water molecules [51]. It is believed that these water molecules play an important role in the adsorption of different gases especially carbon dioxide. This first drop can be linked to the adsorbed gas molecules coming most likely from the air/environment. At around 310°C, CAU-1 framework/structure starts to decompose leading to the end product, probably Al_2O_3 .

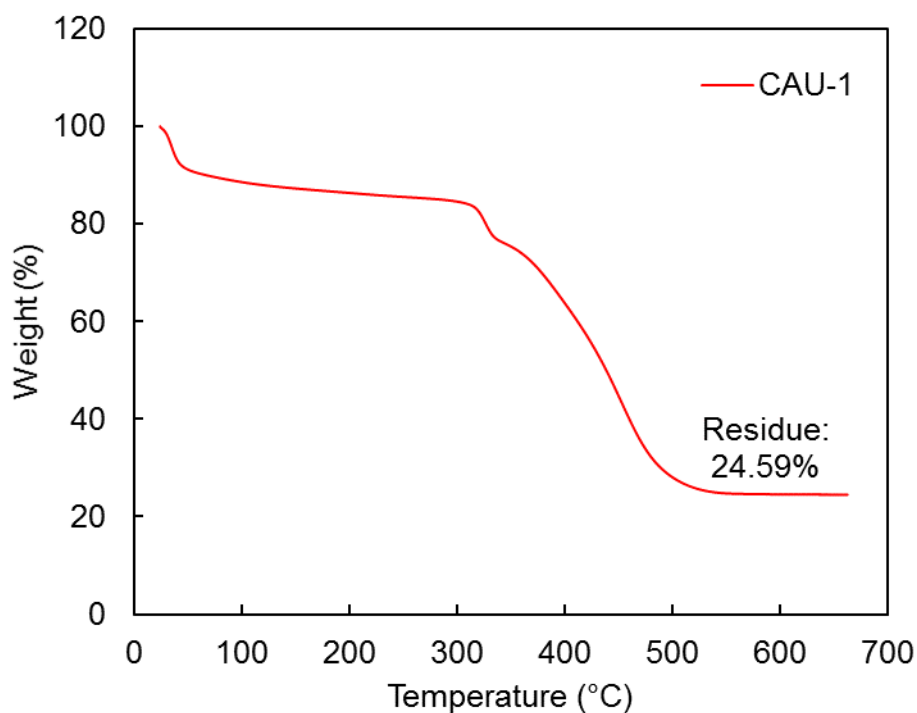


Figure 13. Thermogravimetric analysis of synthesized CAU-1 particles

4.2 Mixed matrix membrane characterization

4.2.1 Microstructure

The cross-section SEM images of PEI membrane and mixed matrix membrane show a spongy structure, Figure 14-17. Spongy structure (closed pore system) in these membranes is achieved by drying the solution in open air after casting on glass plates. If the solution is dried in an oven at a higher temperature (depending on the type of polymer) after casting, the structure is dense (not porous) yielding a lower permeability. High magnification images of 5%, 10% and 15% CAU-1/PEI membranes show the presence of CAU-1 particles embedded in the walls of PEI spongy matrix, (Figure 15b and 17b). The presence of CAU-1 particles within the polymer pore walls enhances the strength of walls and result in the compaction of the sponge structure, therefore, reducing the distance between sponge walls. It is observed that, for 5% and 10% MMMs, the CAU-1 particles are uniformly distributed in the matrix (figure 15-16). However, it is also noticed that 15% CAU-1/PEI membrane contains some agglomerates of CAU-1 particles along with the dispersed particles. These agglomerates have a significant effect on gas permeation of the membrane, as this 15% CAU-1/PEI membrane has shown the highest permeability with the lowest selectivity, as reported in the coming section. It is worth noting that when this membrane is placed in the cell for gas permeation (as mentioned in section 3.4) and tightened to avoid any gas leak, it ruptures/cracks which is normally an indication of fragile nature. These cracks have been observed in the membrane after removing from the cell.

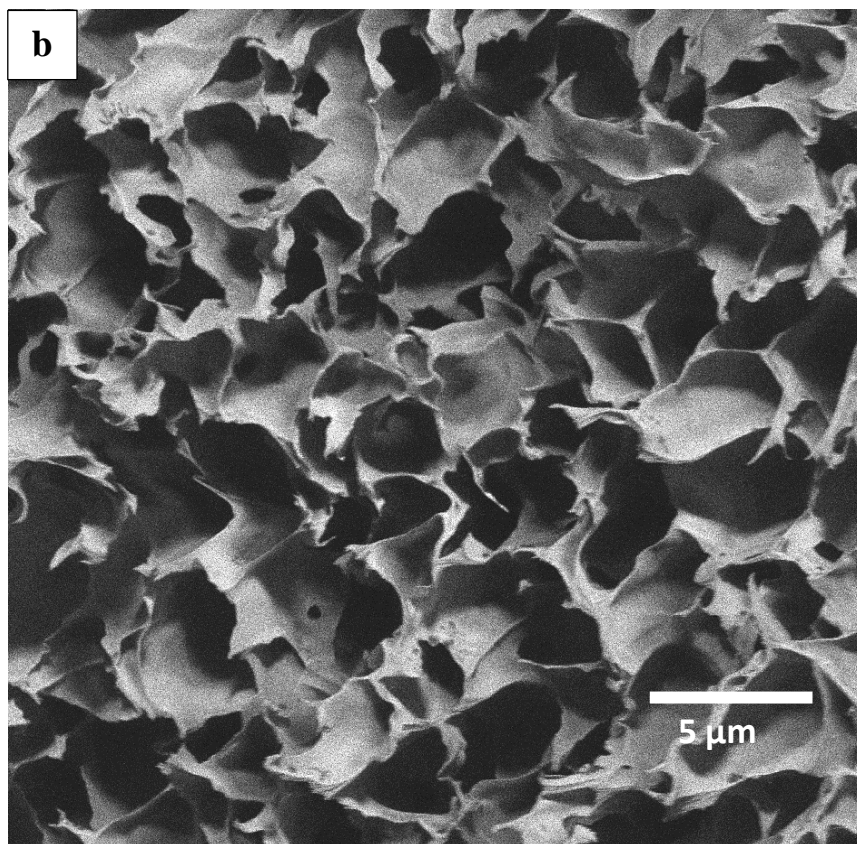
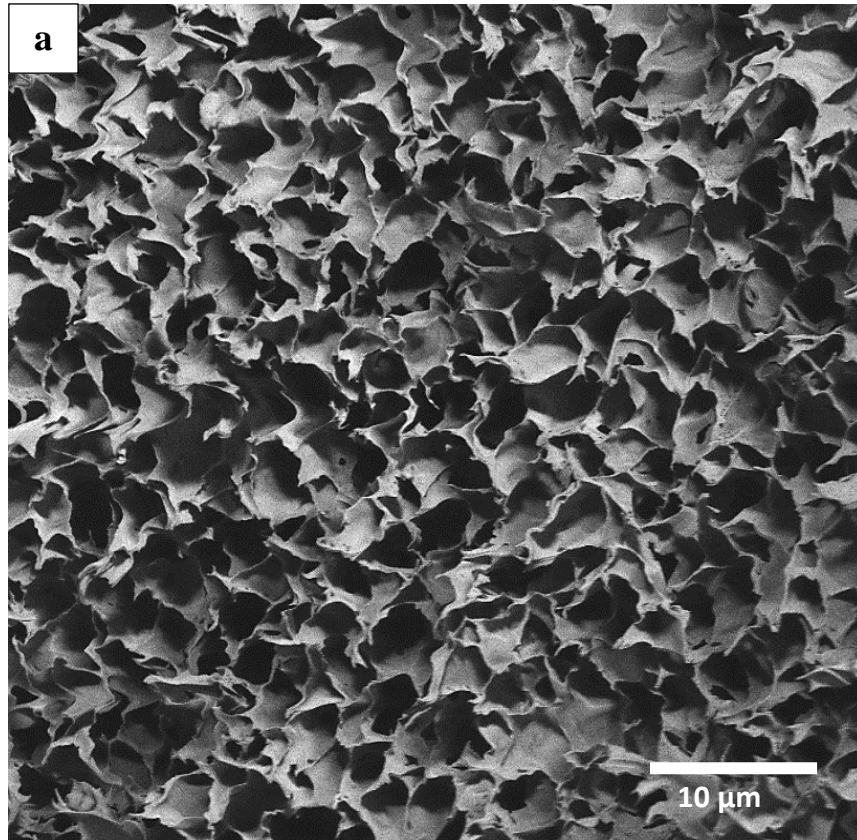


Figure 14. Cross-sectional images of pure PEI membrane showing a spongy morphology a) lower magnification b) higher magnification

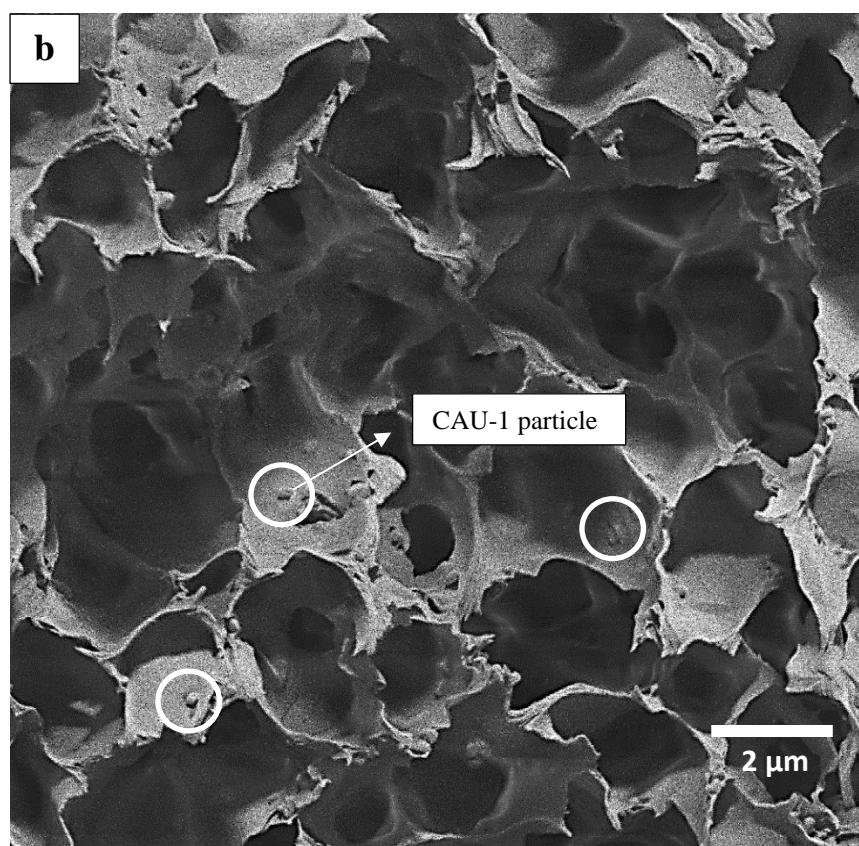
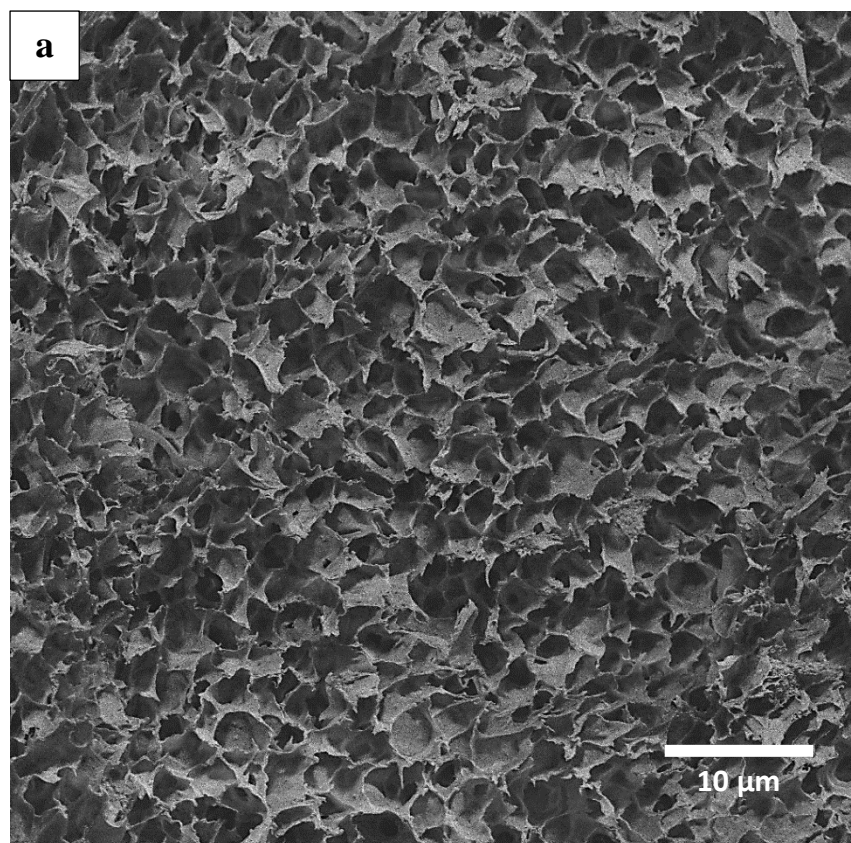


Figure 15. Cross-sectional images of 5% CAU-1/PEI membrane showing a spongy morphology at a) lower magnification b) higher magnification. CAU-1 embedded particles shown inside white circle

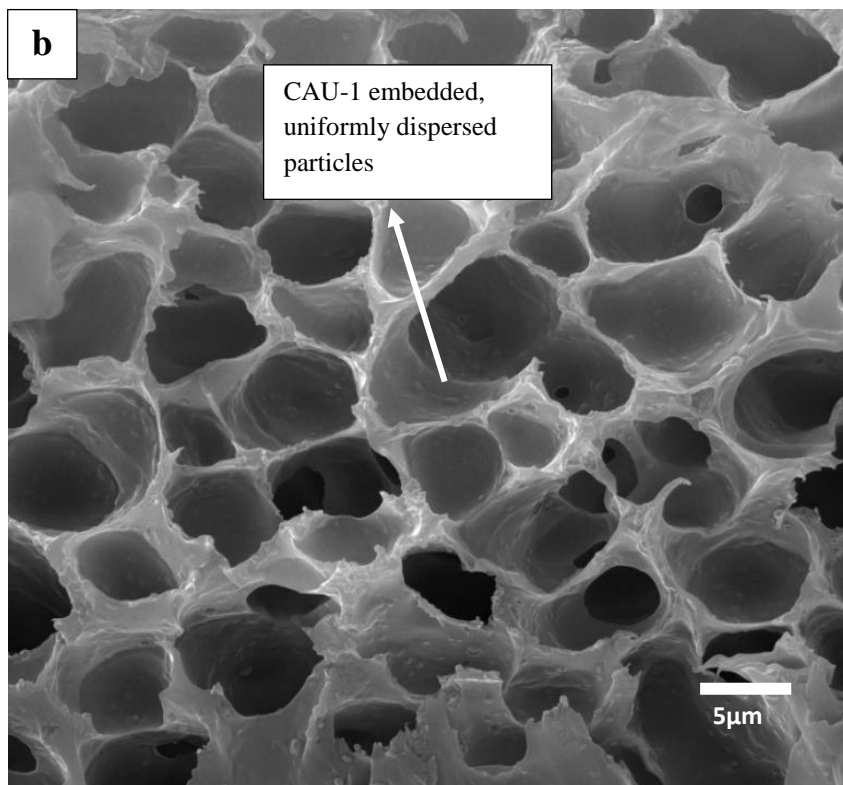
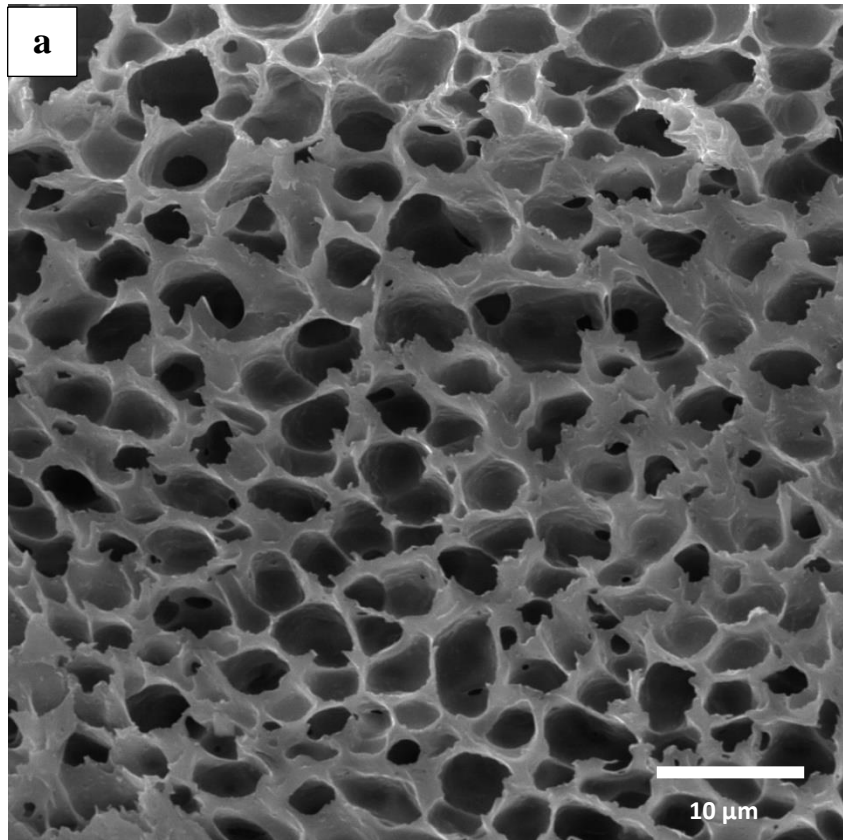


Figure 16. Cross-sectional image of 10% CAU-1/PEI membrane showing a spongy morphology and uniformly dispersed/embedded CAU-1 particles in PEI walls

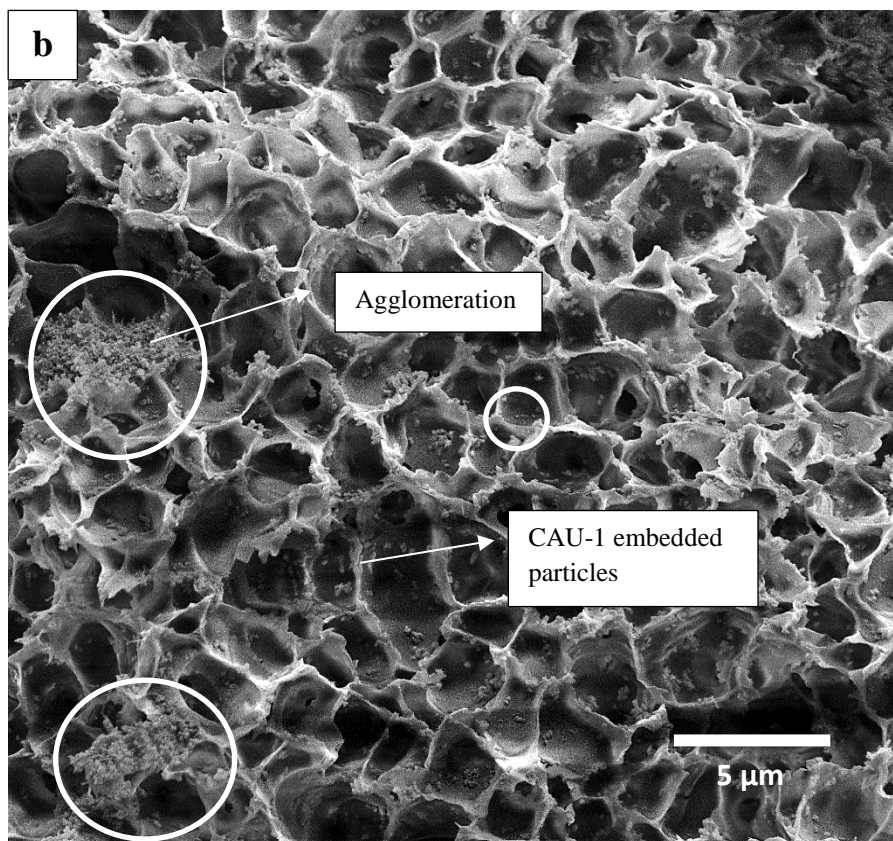
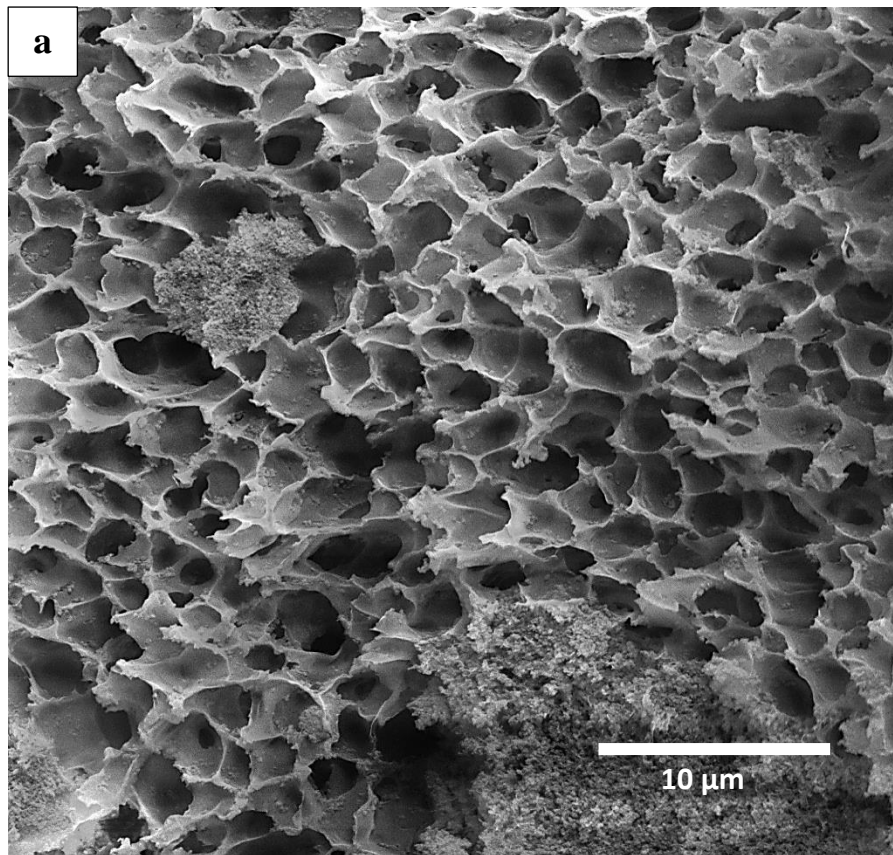


Figure 17. SEM cross-sectional image of 15% CAU-1/PEI membrane showing a spongy morphology at a) lower magnification b) higher magnification. CAU-1 particle agglomeration shown inside orange circle.

4.2.2 X-ray diffraction analysis

The prepared membranes were further characterized using XRD to confirm the existence of CAU-1 particles embedded in PEI matrix. It can be observed (figure 18) that 5%, 10% and 15% CAU-1/PEI mixed matrix membranes contain XRD peaks of CAU-1 particles at a 2θ angle of ~ 7.3 and ~ 10 degrees.

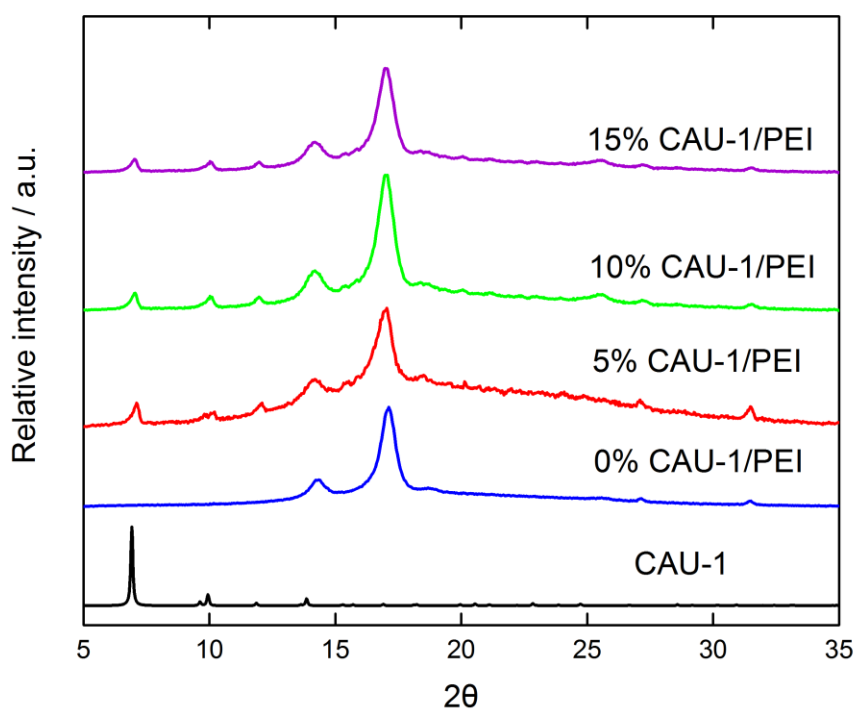


Figure 18. XRD patterns of CAU-1 particles, PEI, 5%, 10% and 15% CAU-1/PEI membranes

4.2.3 Gas Separation

Dense polymeric membranes, unlike symmetric porous spongy membranes, have a very compact structure. During permeation of gases, gas molecules face more resistance in dense membranes as compared to that in spongy membranes. In either case, gas molecules tend to pass through the cavities between the polymeric chains. These cavities, unlike pores, are very minute in size and only allow the molecules to pass through due to the atomic vibrations in polymeric chains. In spongy structured membranes, as shown in Figure 19, when the gas molecules try to pass through the membrane from left to right, they face resistance by the polymeric chains in the walls of the spongy structure/matrix. The rate of diffusion is very slow through the walls. Once the gas molecules have diffused through the wall, they enter a pore where they face no resistance for a distance d shown in Figure 19. And the process continues. However, in the dense membranes where there are no pores, the gas molecules are always facing resistance in diffusing through, resulting in lower permeation rate. When MOF particles are introduced in a spongy polymeric matrix, they tend to embed in the walls of the spongy structure. Since these MOF particles are porous in nature, they provide more space (than polymer) for gas molecules to diffuse at a higher rate. However, the addition of MOF particles into the polymeric matrix results in the rigidity of polymeric chains decreasing the flexibility of the structure **making it harder for gas molecules to pass through membranes due to less vibrations of polymeric chains as described earlier.**

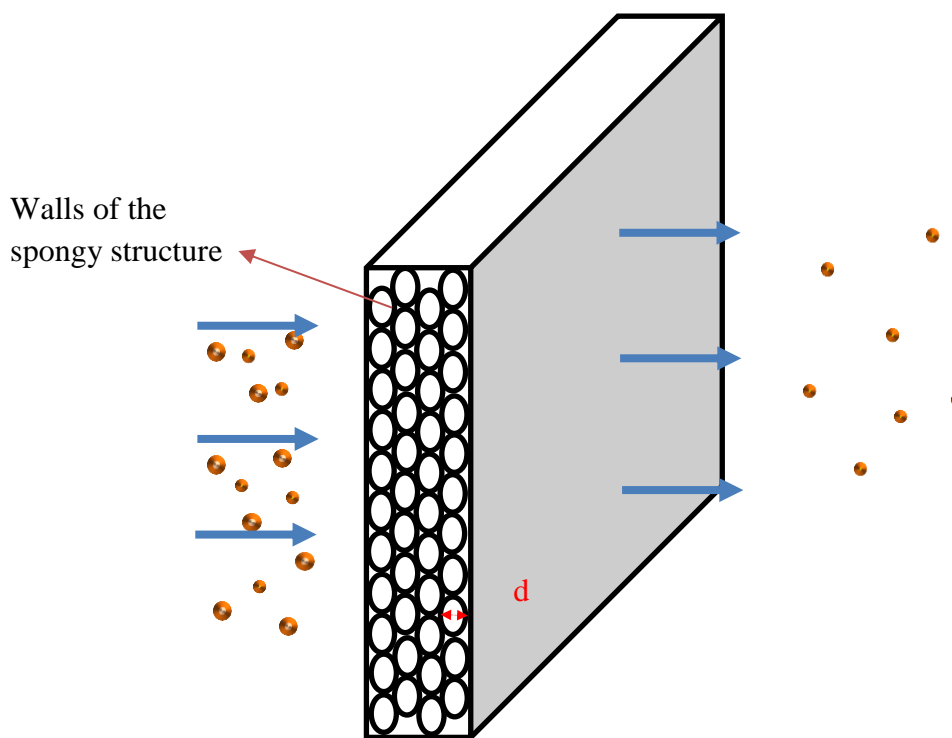


Figure 19. Schematic of gas molecules passing through symmetric spongy porous membrane

All the prepared membranes were tested for gas permeability and gas selectivity in a custom-made equipment. The test results for permeability and selectivity are shown in Tables 5-7, respectively. Gas permeability for several gases, H₂, O₂, N₂, CO₂, and CH₄, was measured. As the concentration of CAU-1 was increased from 0 wt% to 5 wt%, the permeability of gases increased to about 200% (Table 5). This increase in permeability can be attributed to the presence of CAU-1 particles in the mixed matrix membrane which provide an easy way of transfer for gas molecules since the pore window for CAU-1 is in a narrow range of 0.34-0.40 nm. When the concentration was increased to 10 wt%, the permeability of all gases decreased compared to PEI and 5% CAU-1/PEI membranes. This decrease in permeability could possibly be due to enhanced resistance offered by matrix walls as the structure became more rigid when

CAU-1 concentration increased. When the CAU-1 particles concentration was further increased to 15 wt%, the gas permeabilities begin to drop for smaller gas molecules like H₂, remain almost unchanged for medium size gas molecules (O₂, CO₂) and increased for larger gas molecules (N₂, CH₄). This decrease in permeability is explained below. We can elaborate further on the mechanism of gas transfer using solubility and diffusivity of gases in the membrane. However, it is important to notice here that although the permeability increased when the concentration was increased from 0% to 5%, the selectivity of 5% CAU-1/PEI membranes remained almost unchanged. In case of 10% CAU-1/PEI membrane, the permeability of all gases decreased. This decrease may be attributed to the structure getting more rigid with the increase in filler concentration, providing more resistance for larger gas molecules to pass through. At the same time, 10% CAU-1/PEI depicted improved selectivity (higher than that of 5% CAU-1/PEI). When the concentration was increased further to 15%, the selectivity decreased drastically with an increase in permeability, this might be due to the fragile nature of the membrane having higher filler concentration and the presence of large agglomerates which could induce cracks in the membrane.

Table 5. Permeability (Barrer) of mixed matrix membranes with different CAU-1 concentration for different gases at 35°C and 2.05 bar

Membranes	P_{H_2}	P_{O_2}	P_{N_2}	P_{CO_2}	P_{CH_4}
PEI	328	28.2	4.28	91.7	5.22
5 % CAU-1/PEI	633	52	10	193.5	10.5
10% CAU-1/PEI	450	19.3	2	42	1.65
15 % CAU-1/PEI	493.5	53	21	180	21.5

Table 6. Ideal selectivity for different gas pairs for hydrogen separation

Membranes	α (H ₂ /O ₂)	α (H ₂ /N ₂)	α (H ₂ /CO ₂)	α (H ₂ /CH ₄)
PEI	11.63	76.63	3.57	62.84
5 % CAU-1/PEI	12.17	63.3	3.27	60.3
10 % CAU-1/PEI	23.31	180	11.25	281.25
15 % CAU-1/PEI	9.3	23.5	2.75	23

Table 7. Ideal selectivity for CO₂ separation from N₂ and CH₄

Membranes	α (CO ₂ /N ₂)	α (CO ₂ /CH ₄)	α (O ₂ /N ₂)
0 % CAU-1/PEI	21.42	17.58	6.6
5 % CAU-1/PEI	19.35	18.42	5.2
10 % CAU-1/PEI	20	27	9.65
15 % CAU-1/PEI	8.57	8.37	2.5

As discussed earlier, permeability is the product of diffusivity and solubility in polymeric membranes. Table 8 and Table 9 display diffusivity and solubility coefficients as a function of the concentration of CAU-1 concentration in the mixed matrix membranes. When the concentration of CAU-1 is increased in membrane from 0% to 5%, diffusion coefficients are increased for all gases by almost 100%. But the solubility coefficients remain almost unchanged for all gases except for CO₂. Solubility coefficient for CO₂ is increased in this case which is as expected. The reason for the increase in solubility coefficient of CO₂ is the presence of CAU-1 particles which have an affinity towards the CO₂ molecules as discussed in 5.1.3. To be clear, CO₂ molecules are polar in nature and CAU-1 framework contains amino functional groups which attract CO₂ molecule. The presence of hydroxyl groups in CAU-1 framework also

shows an affinity towards CO₂ molecules. Therefore, solubility coefficient increases by adding more CAU-1 particles in the membrane given that the matrix structure remains the same.

Table 8. Diffusivity coefficient of different gases as a function of CAU-1 concentration

Membranes	Diffusivity Coefficient (10 ⁻⁷ cm ² /s)				
	H ₂	O ₂	N ₂	CO ₂	CH ₄
PEI	20.1	1.74	0.67	1.54	0.623
5 % CAU-1/PEI	40.1	3.82	1.46	2.39	1.19
10 % CAU-1/PEI	33.9	1.33	1.15	0.605	0.18
15 % CAU-1/PEI	23.2	3.17	2.64	2	2.3

Table 9. Solubility coefficient of different gases as a function of CAU-1 concentration

Membranes	Solubility Coefficient (10 ⁷ cm ³ (STP)/cm ³ cmHg)				
	H ₂	O ₂	N ₂	CO ₂	CH ₄
PEI	16.9	16.3	6.67	59.5	8.53
5 % CAU-1/PEI	15.8	13.6	6.8	81.1	8.96
10 % CAU-1/PEI	13.4	15.1	1.90	69.6	9.05
15 % CAU-1/PEI	21.4	16.8	8.16	98	8.7

Figure 20 shows diffusion coefficient of H₂, O₂, N₂, CO₂ and CH₄ gases for the developed membranes as a function of Lennard-Jones diameter of the mentioned gas molecules. The diffusion of these gases through PEI and MMMs depends on the size of the gas molecules. As the molecular size of gas molecules increases, the diffusion coefficient decreases given the window aperture of the passage remains the same. CAU-1 has pore window aperture of 0.3-0.4 nm. Smaller molecules like H₂ can pass

easily through these pores. However, larger molecules have resistance passing through the membrane as there might be some interaction between the gas molecules and pore windows. A small quantity of larger molecules can overcome this interaction under the action of pressure and flexibility of window, passing through the pore window. The interaction between gas molecules and membrane is always controlled by the gas adsorption and diffusion. It is also important to notice that the closer the diffusion coefficients are to the trend line (linear fit of diffusion coefficient points), the more the gas transport follows the diffusion model. The disparity of diffusion coefficients from the trend line means that there is some other phenomenon also going on besides diffusion for gas transport. This is the reason to believe that 15% CAU-1/PEI membrane is defective since diffusion coefficients are very close to the respective trend line unlike other membranes.

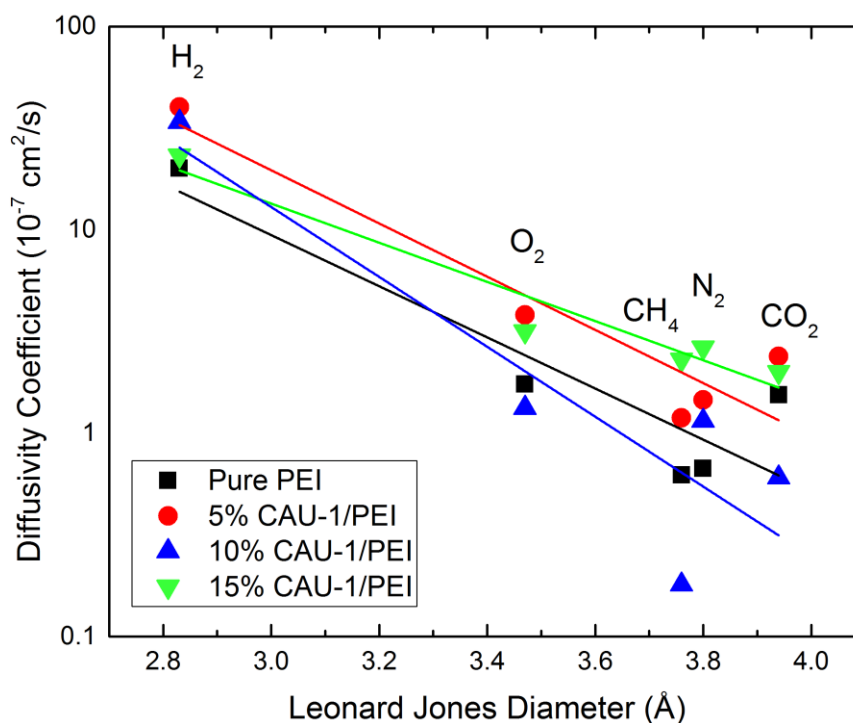


Figure 20. Diffusion coefficients versus Lennard-Jones diameter

4.2.4 Comparative analysis

Robeson's upper bound correlation states that there is usually a trade-off between permeability and gas selectivity of a polymeric membrane. Permeability for H₂, O₂, N₂, CO₂, and CH₄ was tested and used to calculate ideal selectivity for different gas pairs; H₂/N₂, H₂/CO₂, H₂/CH₄, O₂/N₂, CO₂/N₂, and CO₂/CH₄. The permeability and selectivity measured for our developed membranes are plotted against the data obtained in literature for mixed matrix membrane using PEI as a matrix. It is observed from Figure 21-22 that 5% CAU-1/PEI shows almost similar selectivity to the pure PEI for CO₂/CH₄ and CO₂/N₂ gas pairs but with enhanced CO₂ permeability would make such membrane more appealing to the gas separation industries. For 10% CAU-1/PEI membrane, selectivity is increased but permeability of CO₂ is decreased. For H₂ separation from N₂, CO₂, or CH₄, permselectivity for both 5% and 10% CAU-1/PEI lies above the Robeson upper bound (2008), where 10% CAU-1/PEI membrane shows a significantly higher selectivity than 5% CAU-1/PEI membrane as shown in Figure 23-25.

Compared to literature, 10% CAU-1/PEI mixed matrix membrane shows the highest permselectivity for H₂ separation as indicated in figures 23-25. The significant part of this work is that the permselectivity measured for 5% and 10% CAU-1/PEI mixed matrix membranes is closer to the Robeson upper bound curve for CO₂ removal (from N₂, or CH₄) and above the Robeson upper bound for H₂ separation (from O₂, N₂, CH₄, or CO₂).

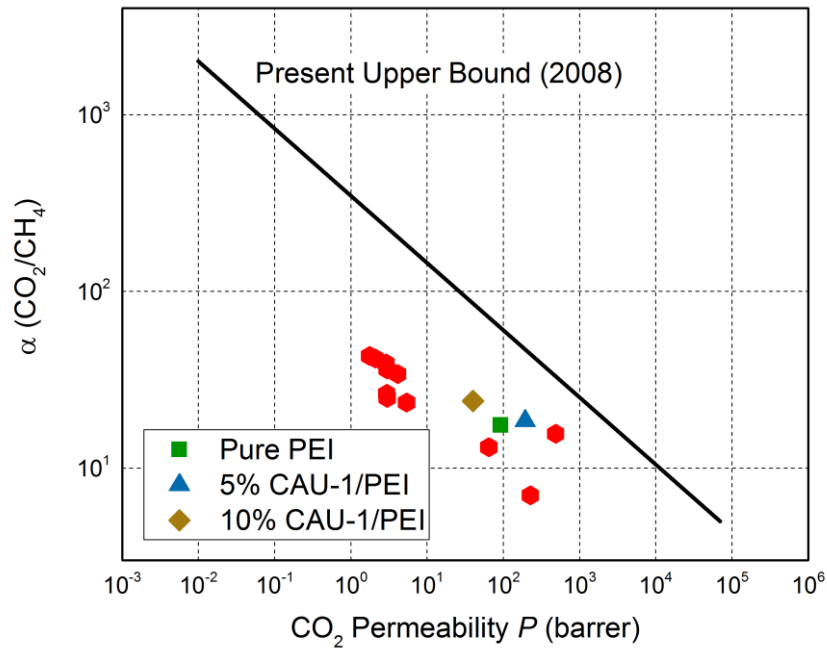


Figure 21. Correlation between P_{CO_2} and $\alpha (CO_2/CH_4)$ of Pure PEI (green), 5% CAU-1/PEI MMM (Blue), and 10% CAU-1/PEI MMM (brown) compared to Robeson Upper Bound (Black line) and reported membranes (Red)

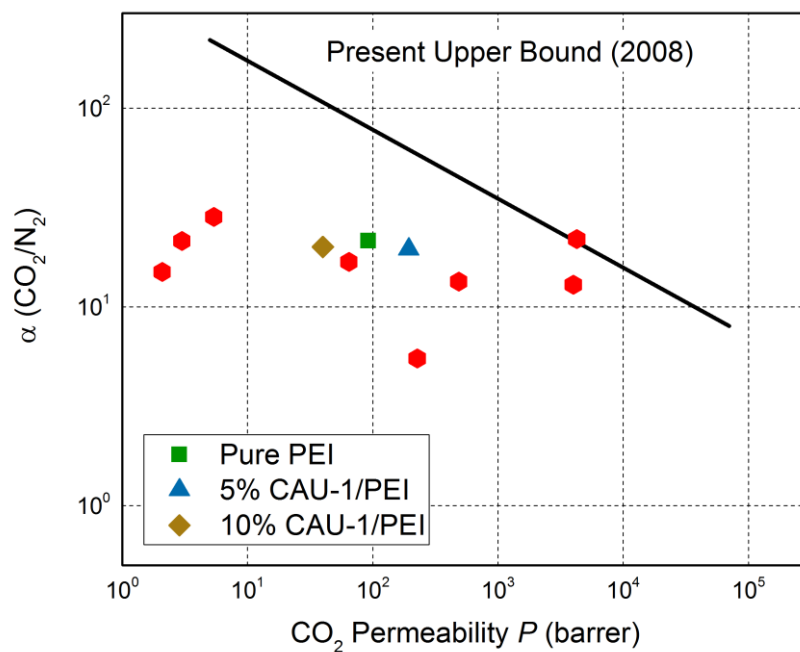


Figure 22. Correlation between P_{CO_2} and $\alpha (CO_2/N_2)$ of Pure PEI (green), 5% CAU-1/PEI MMM (Blue), and 10% CAU-1/PEI MMM (brown) compared to Robeson Upper Bound (Black line) and reported membranes (Red)

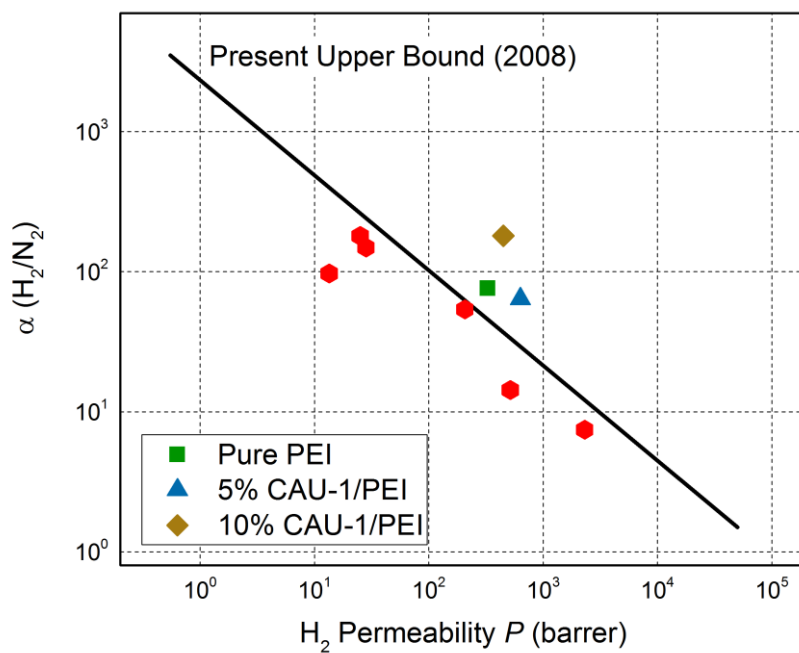


Figure 23. Correlation between P_{H_2} and $\alpha (H_2/N_2)$ of Pure PEI (green), 5% CAU-1/PEI MMM (Blue), and 10% CAU-1/PEI MMM (brown) compared to Robeson Upper Bound (Black line) and reported membranes (Red)

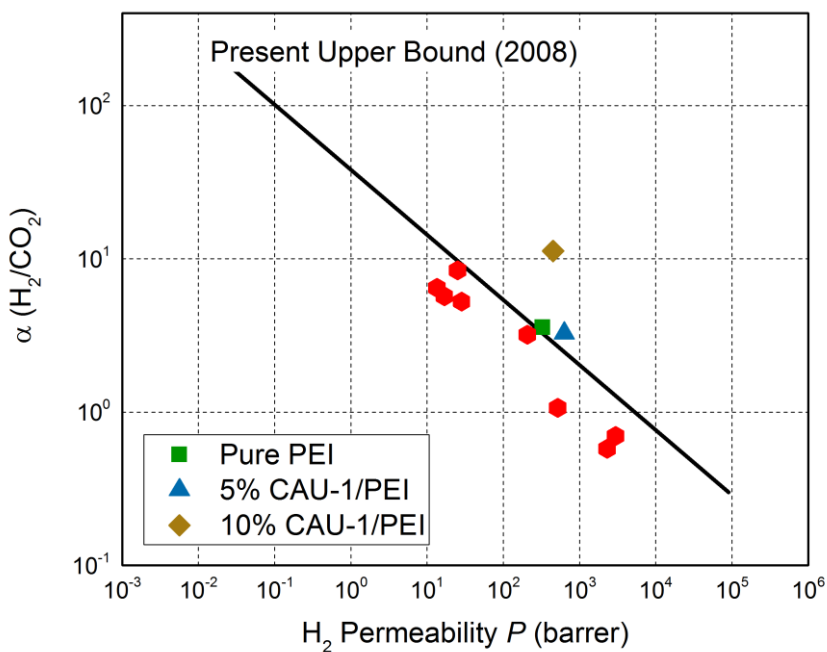


Figure 24. Correlation between P_{H_2} and $\alpha (H_2/CO_2)$ of Pure PEI (green), 5% CAU-1/PEI MMM (Blue), and 10% CAU-1/PEI MMM (brown) compared to Robeson Upper Bound (Black line) and reported membranes (Red)

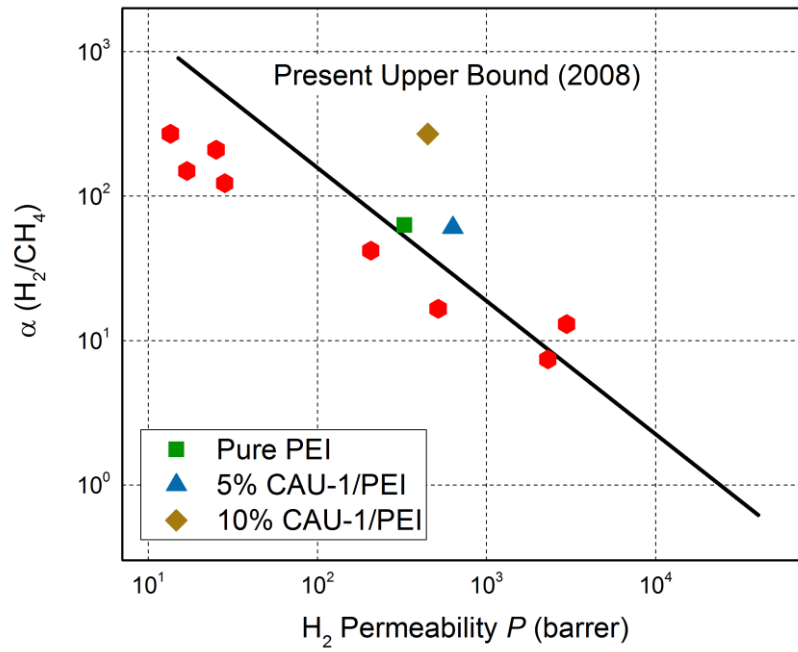


Figure 25. Correlation between P_{H_2} and α (H₂/CH₄) of Pure PEI (green), 5% CAU-1/PEI MMM (Blue), and 10% CAU-1/PEI MMM (brown) compared to Robeson Upper Bound (Black line) and reported membranes (Red)

CHAPTER 5

CONCLUSIONS AND RECOMMENDATIONS

A novel mixed matrix membrane composed of PEI matrix reinforced with CAU-1 particles has been developed and tested for gas separation. The conclusions can be summarized as follows:

- 1) CAU-1 particles are synthesized using solvothermal technique with an average particle size of 300-500 nm and BET surface area of 1149 m²/g.
- 2) Mixed matrix membranes are fabricated with varying concentration (5%, 10%, and 15%) by solution and knife casting technique, possessing a symmetrical spongy porous structure, with thickness of ~150 micron.
- 3) The 5% CAU-1/PEI mixed matrix membrane illustrates improved gas permeability compared to PEI membrane without any change in selectivity, while permselectivity is closer to the Robeson upper bound for CO₂ removal from N₂ or CH₄.
- 4) For H₂ separation from O₂, N₂, CO₂ and CH₄, the permselectivity for 5% CAU-1/PEI membrane crosses the upper bound. The permeability for H₂, O₂, N₂, CO₂ and CH₄ has increased from 328, 28.2, 4.28, 91.7 and 5.22 barrer to 633, 52, 10, 193.5 and 10.5 barrer respectively with selectivity for H₂/N₂, H₂/CO₂, CO₂/N₂ and CO₂/CH₄ being unchanged.
- 5) For 10% CAU-1/PEI membrane, the permeability decreases in comparison to 5% CAU-1/PEI membrane but with a significant improvement in selectivity of H₂/O₂, H₂/N₂, H₂/CO₂, and H₂/CH₄. The decrease in permeability can be

attributed to the rigidification of the spongy structure due to increased CAU-1 particle concentration.

- 6) Further increase in concentration of CAU-1 particles to 15 wt% has caused agglomeration, yielding cracks resulting in a significant drop in selectivity.

Future work recommendations are

- 1) Functionalizing CAU-1 crystals to reduce the pore size as well as increase affinity towards certain gases.
- 2) Development of membranes with CAU-1 and functionalized CAU-1 particles without the PDMS treatment.
- 3) Evaluation of the gas separation performance of water-soaked, then dried CAU-1/PEI membranes to study whether the water affects the stability or gas separation performance of mixed matrix membranes.

References

- [1] D. L. Hartmann, A. M. G. K. Tank, and M. Rusticucci, “2: Observations: Atmosphere and Surface,” 2013.
- [2] S. Borenstein, “Earth is a wilder, warmer place since last climate deal made,” 2015.
- [3] “CLIMATE CHANGE 2014: Synthesis Report. Summary for Policymakers,” 2015.
- [4] A. Buis, K. Ramsayer, and C. Rasmussen, “A Breathing Planet, Off Balance,” 2015.
- [5] P. U. Clark, “Abrupt Climate Change. A Report by the U.S. Climate Change Science Program and the Subcommittee on Global Change Research,” 2008.
- [6] “Ocean Acidification, in: Ch. 2. Our Changing Climate, in NCADAC,” 2013.
- [7] *Summary, National Research Council*. 2011, pp. 14–19.
- [8] C. A. Scholes, G. W. Stevens, and S. E. Kentish, “Membrane gas separation applications in natural gas processing,” *Fuel*, vol. 96, pp. 15–28, 2012.
- [9] IPCC, “Synthesis Report Summary for Policymakers, Section 4: Adaptation and Mitigation Options,” 2007.
- [10] “UNFCCC Glossary of Climate Change Acronyms,” 2010.
- [11] D. A. Farber, “Adapting to Climate Change : Who Should Pay?,” *UC Berkeley Public Law Theory*, 2007.

- [12] S. H. Schneider *et al.*, “Executive summary. In (book chapter): Chapter 19: Assessing Key Vulnerabilities and the Risk from Climate Change. In: Climate Change 2007: Impacts, Adaptation and Vulnerability. Contribution of Working Group II to the Fourth Assessment Report of the Inter,” 2007.
- [13] T. F. Stocker *et al.*, “Climate Change 2013: The Physical Science Basis. Summary for Policy Makers,” 2013.
- [14] “Cool Inventions,” *Institution of Chemical Engineers*, 2010. .
- [15] W. H. Isalski, “Monograph on Cryogenics,” *New York: Oxford University Press*, no. Separation of Gases, pp. 228–233, 1989.
- [16] O. M. Yaghi, M. O’Keeffe, N. W. Ockwig, H. K. Chae, M. Eddaoudi, and J. Kim, “Reticular synthesis and the design of new materials.,” *Nature*, vol. 423, no. 6941, pp. 705–14, Jun. 2003.
- [17] X.-C. Huang, Y.-Y. Lin, J.-P. Zhang, and X.-M. Chen, “Ligand-Directed Strategy for Zeolite-Type Metal–Organic Frameworks: Zinc(II) Imidazolates with Unusual Zeolitic Topologies,” *Angew. Chemie Int. Ed.*, vol. 45, no. 10, pp. 1557–1559, Feb. 2006.
- [18] H. Hayashi, A. P. Côté, H. Furukawa, M. O’Keeffe, and O. M. Yaghi, “Zeolite A imidazolate frameworks,” *Nat. Mater.*, vol. 6, no. 7, pp. 501–506, Jul. 2007.
- [19] G. Férey, B. F. Hoskins, and R. Robson, “Hybrid porous solids: past, present, future,” *Chem. Soc. Rev.*, vol. 37, no. 1, pp. 191–214, 2008.
- [20] C. M. Lew, R. Cai, and Y. Yan, “Zeolite Thin Films: From Computer Chips to Space Stations,” *Acc. Chem. Res.*, vol. 43, no. 2, pp. 210–219, Feb. 2010.

- [21] M. D. Allendorf *et al.*, “Stress-induced chemical detection using flexible metal-organic frameworks,” *J. Am. Chem. Soc.*, vol. 130, no. 44, pp. 14404–5, Nov. 2008.
- [22] M. C. McCarthy, V. Varela-Guerrero, G. V Barnett, and H.-K. Jeong, “Synthesis of zeolitic imidazolate framework films and membranes with controlled microstructures,” *Langmuir*, vol. 26, no. 18, pp. 14636–41, Sep. 2010.
- [23] A. Phan, C. J. Doonan, F. J. Uribe-Romo, C. B. Knobler, M. O’Keeffe, and O. M. Yaghi, “Synthesis, structure, and carbon dioxide capture properties of zeolitic imidazolate frameworks,” *Acc. Chem. Res.*, vol. 43, no. 1, pp. 58–67, Jan. 2010.
- [24] Y. Li, F. Liang, H. Bux, W. Yang, and J. Caro, “Zeolitic imidazolate framework ZIF-7 based molecular sieve membrane for hydrogen separation,” *J. Memb. Sci.*, vol. 354, no. 1–2, pp. 48–54, 2010.
- [25] J. Nan, X. Dong, W. Wang, W. Jin, and N. Xu, “Step-by-Step Seeding Procedure for Preparing HKUST-1 Membrane on Porous γ -Alumina Support,” pp. 4309–4312, 2011.
- [26] M. Askari and T.-S. Chung, “Natural gas purification and olefin/paraffin separation using thermal cross-linkable co-polyimide/ZIF-8 mixed matrix membranes,” *J. Memb. Sci.*, vol. 444, pp. 173–183, 2013.
- [27] H. Bux, F. Liang, Y. Li, J. Cravillon, and M. Wiebcke, “Zeolitic Imidazolate Framework Membrane with Molecular Sieving Properties by Microwave-Assisted Solvothermal Synthesis,” pp. 16000–16001, 2009.

- [28] A. Huang, H. Bux, F. Steinbach, and J. Caro, "Molecular-Sieve Membrane with Hydrogen Permselectivity: ZIF-22 in LTA Topology Prepared with 3-Aminopropyltriethoxysilane as Covalent Linker," *Angew. Chemie Int. Ed.*, vol. 49, no. 29, pp. 4958–4961, Jun. 2010.
- [29] Y. Liu, E. Hu, E. A. Khan, and Z. Lai, "Synthesis and characterization of ZIF-69 membranes and separation for CO₂/CO mixture," *J. Memb. Sci.*, vol. 353, no. 1, pp. 36–40, 2010.
- [30] X. Dong, K. Huang, and S. Liu, "Synthesis of zeolitic imidazolate framework-78 molecular-sieve membrane: defect formation and elimination," *J. Mater. Chem.*, vol. 22, no. 36, p. 19222, 2012.
- [31] A. Huang, N. Wang, C. Kong, and J. Caro, "Organosilica-Functionalized Zeolitic Imidazolate Framework ZIF-90 Membrane with High Gas-Separation Performance," *Angew. Chemie Int. Ed.*, vol. 51, no. 42, pp. 10551–10555, Oct. 2012.
- [32] A. Huang, W. Dou, and J. Caro, "Steam-Stable Zeolitic Imidazolate Framework ZIF-90 Membrane with Hydrogen Selectivity through Covalent Functionalization," *J. Am. Chem. Soc.*, vol. 132, no. 44, pp. 15562–15564, Nov. 2010.
- [33] F. Cacho-Bailo, G. Caro, and M. Etxeberria-Benavides, "High selectivity ZIF-93 hollow fiber membranes for gas separation," *Chem. Commun.*, vol. 51, no. 56, pp. 11283–11285, 2015.
- [34] A. Huang, Y. Chen, N. Wang, Z. Hu, J. Jiang, and J. Caro, "A highly permeable and selective zeolitic imidazolate framework ZIF-95 membrane for

- H₂/CO₂ separation.,” *Chem. Commun. (Camb)*., vol. 48, no. 89, pp. 10981–3, Nov. 2012.
- [35] N. Wang, Y. Liu, and Z. Qiao, “Polydopamine-based synthesis of a zeolite imidazolate framework ZIF-100 membrane with high H₂/CO₂ selectivity,” *J. Mater. Chem. A*, vol. 3, no. 8, pp. 4722–4728, 2015.
- [36] H. Furukawa, M. O. Keeffe, O. M. Yaghi, B. Wang, and A. P. Co, “Colossal cages in zeolitic imidazolate frameworks as selective carbon dioxide reservoirs,” vol. 453, no. May, pp. 207–212, 2008.
- [37] J. Yao, D. Dong, D. Li, L. He, G. Xu, and H. Wang, “ChemComm Contra-diffusion synthesis of ZIF-8 films on a polymer substrate w,” pp. 2559–2561, 2011.
- [38] P. V. Kortunov *et al.*, “Intracrystalline Diffusivities and Surface Permeabilities Deduced from Transient Concentration Profiles: Methanol in MOF Manganese Formate,” *J. Am. Chem. Soc.*, vol. 129, no. 25, pp. 8041–8047, Jun. 2007.
- [39] E. Biemmi, A. Darga, N. Stock, and T. Bein, “Direct growth of Cu₃(BTC)₂(H₂O)₃·xH₂O thin films on modified QCM-gold electrodes – Water sorption isotherms,” *Microporous Mesoporous Mater.*, vol. 114, no. 1, pp. 380–386, 2008.
- [40] S. Hermes, D. Zacher, A. Baunemann, C. Wöll, and R. A. Fischer, “Selective Growth and MOCVD Loading of Small Single Crystals of MOF-5 at Alumina and Silica Surfaces Modified with Organic Self-Assembled Monolayers †,” *Chem. Mater.*, vol. 19, no. 9, pp. 2168–2173, May 2007.
- [41] S. Hermes, F. Schröder, R. Chelmoski, C. Wöll, and R. A. Fischer, “Selective

- Nucleation and Growth of Metal–Organic Open Framework Thin Films on Patterned COOH/CF₃-Terminated Self-Assembled Monolayers on Au(111),” *J. Am. Chem. Soc.*, vol. 127, no. 40, pp. 13744–13745, Oct. 2005.
- [42] E. Biemmi, C. Scherb, and T. Bein, “Oriented growth of the metal organic framework Cu₃(BTC)₂(H₂O)₃.xH₂O tunable with functionalized self-assembled monolayers,” *J. Am. Chem. Soc.*, vol. 129, no. 26, pp. 8054–5, Jul. 2007.
- [43] M. Arnold, P. Kortunov, D. J. Jones, Y. Nedellec, J. Kärger, and J. Caro, “Oriented Crystallisation on Supports and Anisotropic Mass Transport of the Metal-Organic Framework Manganese Formate,” *Eur. J. Inorg. Chem.*, vol. 2007, no. 1, pp. 60–64, Jan. 2007.
- [44] J. Gascon, S. Aguado, and F. Kapteijn, “Manufacture of dense coatings of Cu₃(BTC)₂ (HKUST-1) on α -alumina,” *Microporous Mesoporous Mater.*, vol. 113, no. 1, pp. 132–138, 2008.
- [45] O. Shekhah *et al.*, “Step-by-Step Route for the Synthesis of Metal–Organic Frameworks,” *J. Am. Chem. Soc.*, vol. 129, no. 49, pp. 15118–15119, Dec. 2007.
- [46] W. Liang and D. M. D’Alessandro, “Microwave-assisted solvothermal synthesis of zirconium oxide based metal–organic frameworks,” *Chem. Commun.*, vol. 49, no. 35, p. 3706, 2013.
- [47] R. Ameloot, L. Stappers, J. Fransaer, L. Alaerts, B. F. Sels, and D. E. De Vos, “Patterned Growth of Metal-Organic Framework Coatings by Electrochemical Synthesis,” *Chem. Mater.*, vol. 21, no. 13, pp. 2580–2582, Jul. 2009.
- [48] L. M. Robeson, “The upper bound revisited,” *J. Memb. Sci.*, vol. 320, no. 1, pp.

390–400, 2008.

- [49] R. Mahajan, R. Burns, M. Schaeffer, and W. J. Koros, “Challenges in forming successful mixed matrix membranes with rigid polymeric materials,” *J. Appl. Polym. Sci.*, vol. 86, no. 4, pp. 881–890, Oct. 2002.
- [50] T.-S. Chung, L. Y. Jiang, Y. Li, and S. Kulprathipanja, “Mixed matrix membranes (MMMs) comprising organic polymers with dispersed inorganic fillers for gas separation,” *Prog. Polym. Sci.*, vol. 32, no. 4, pp. 483–507, Apr. 2007.
- [51] T. Ahnfeldt *et al.*, “[Al₄(OH)₂(OCH₃)₄(H₂N-Bdc)₃] \cdot xH₂O: A 12-connected porous metal-organic framework with an unprecedented aluminum-containing brick,” *Angew. Chemie - Int. Ed.*, vol. 48, no. 28, pp. 5163–5166, 2009.
- [52] M. G. García, J. Marchese, and N. A. Ochoa, “Effect of the particle size and particle agglomeration on composite membrane performance,” *J. Appl. Polym. Sci.*, vol. 118, no. 4, p. n/a-n/a, Jun. 2010.
- [53] T. H. Bae, J. S. Lee, W. Qiu, W. J. Koros, C. W. Jones, and S. Nair, “A high-performance gas-separation membrane containing submicrometer-sized metal-organic framework crystals,” *Angew. Chemie - Int. Ed.*, vol. 49, no. 51, pp. 9863–9866, 2010.
- [54] Y. Dai, J. R. Johnson, O. Karvan, D. S. Sholl, and W. J. Koros, “Ultem[®]/ZIF-8 mixed matrix hollow fiber membranes for CO₂/N₂ separations,” *J. Memb. Sci.*, vol. 401–402, pp. 76–82, 2012.
- [55] X. Y. Chen, V.-T. Hoang, D. Rodrigue, and S. Kaliaguine, “Optimization of continuous phase in amino-functionalized metal–organic framework (MIL-53)

- based co-polyimide mixed matrix membranes for CO₂/CH₄ separation,” *RSC Adv.*, vol. 3, no. 46, p. 24266, 2013.
- [56] C. Duan *et al.*, “Enhanced gas separation properties of metal organic frameworks/ polyetherimide mixed matrix membranes,” *J. Appl. Polym. Sci.*, vol. 131, no. 17, pp. 8828–8837, 2014.
- [57] M. Arjmandi, M. Pakizeh, and O. Pirouzram, “The role of tetragonal-metal-organic framework-5 loadings with extra ZnO molecule on the gas separation performance of mixed matrix membrane,” *Korean J. Chem. Eng.*, vol. 32, no. 6, pp. 1178–1187, 2015.
- [58] B. A. Al-Maythaly *et al.*, “Tuning the Interplay between Selectivity and Permeability of ZIF-7 Mixed Matrix Membranes,” *ACS Appl. Mater. Interfaces*, vol. 9, no. 39, pp. 33401–33407, Oct. 2017.

Vitae

Name	Omar Waqas Saadi
Nationality	Pakistani
Date of Birth	3/12/1993
Email	uwsaadi@gmail.com
Address	Street # 2, Muslim Colony Sadiqabad (Postal Code: 64350) District Rahim Yar Khan, Pakistan,
Academic Background	BS in Materials Science and Engineering